Radar and Stereoscopy

The Canada Centre for Remote Sensing is pleased to offer this tutorial on Radar and Stereoscopy authored by **Dr. Thierry Toutin** and **Corinna Vester**. Intended as an overview at a senior high school or early university level, this module touches on relevant aspects of stereoscopy and radar remote sensing, with special focus on the use of RADARSAT imagery.

For teachers and students we have more details and suggestions for using the tutorial (including the availability of downloadable version 1.2 for use off-line). Our RADARSAT-1 Stereo Advisor can be used as an additional teaching tool.

We welcome comments and suggestions on this module.

Contact

To contact the authors, please email: Thierry Toutin

Permission for Use

1. Introduction

Not so long ago, a hill top view was the largest vista from which to observe nature's workings. Discoveries in optics, photography and flight have allowed us to see the Earth as never before. Advanced methods in computing and signal processing technologies et cetera have enabled us to increase our ability to visualize and perceive the Earth's surface. Today, Earth observation satellites orbit our planet collecting data needed to produce images which allow us to monitor, understand and plan the use of our world's resources.

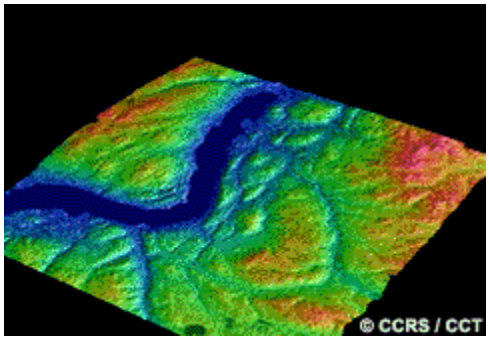

Throughout history, humans have tried to represent what they saw and understood through images. Everything from cave walls, to canvases, to computer screens have been used to express perception of our surroundings. Maps have been one way to show the relationship between humans and their environment. Towns, roads, rivers, mountains, valleys, and where the land meets the sea, have been drawn in an organized fashion for centuries. Mapmakers have always sought ways in which to represent both the location and the three **dimensional shape of land.**

The Third Dimension

Mapmakers and other illustrators have traditionally used rendering techniques such as shading, overlapping and perspective views to give an impression of three dimensionality. In the last 200 years, many advances in representing three dimensions have been made. Stereo models, anaglyphs, chromo-stereoscopic images and holograms can provide three-dimensional (3-D) information about our planet that flat, two-dimensional (2-D) images can not. Why is it important that the third dimension be conveyed? Humans are naturally able to see in three dimensions. The 'naturalness' of a 3-D representation of reality enhances our ability to interpret 2-D imagery. Cartographers, engineers, geologists, hydrologists, and other scientists use 3-D viewing methods, such as stereo viewing of aerial photos and satellite images, in order to better understand the Earth's surface. Representation of the third dimension supplies important information about relationships between land shape and structure, slopes, water ways, surface material and vegetative growth.

Stereo viewing of two 2-D images has been used since the mid 1800's. Stereoscopes are still widely used throughout the world. They are much less expensive and much more portable than computer hardware and software. Even though automatic methods to extract quantitative information from a stereo pair have been developed, qualitative interpretation is best handled by people skilled in stereo viewing. For many users and applications, a stereoscope and a stereopair represent the most efficient way of getting a large amount of information about an area of the Earth quickly and inexpensively.

About this training package

The following sections compose a training package designed to demonstrate the feasibility and potential of stereoscopy with respect to RADARSAT data. RADARSAT,

Canada's first Earth observation satellite, was launched in November 1995. It is a C-band SAR satellite with the ability to provide imagery of any part of the Earth's surface, in any climatic conditions, and by day or night. RADARSAT imagery is well suited to be used in stereo because it can be collected from different look directions, beam modes, beam positions, and at resolutions fine enough to provide a good level of detail of the Earth's surface. This training package has been divided into six sections which are intended to provide the background needed to fulfil the goal of this manual which is How to Use RADARSAT Data in Stereo. The manual is not intended to review and discuss in great detail the topics in each section. A bibliography has been provided for those interested in pursuing any of the topics in greater detail.

2. Visual ability in 3-D

Humans receive information about their surroundings through **five physical sensors**, the eyes, ears, nose, taste receptors and sensory receptors in the skin. Of our five senses, **sight** provides us with the most information about our environment. Two eyes can transmit information at 4.3 million bits/sec while the maximum reception of sound by two ears is 8000 bits/sec.

Human vision is a complex and sophisticated system involving physiological, biochemical, neurological and psychological processes. The following is a simplified description of visual mechanics, the relationship between vision and perception, and the factors that enable us to perceive depth.

2.1 Visual Mechanics

Our **eyes** gather information by processing light reflected from or emitted by objects. Light rays enter the cornea and are refracted by its curved surface. As a result the light rays are squeezed together. This allows them to enter the pupil. The iris regulates the amount of light entering the pupil. Bright light causes the iris to contract and dim light causes it to dilate.

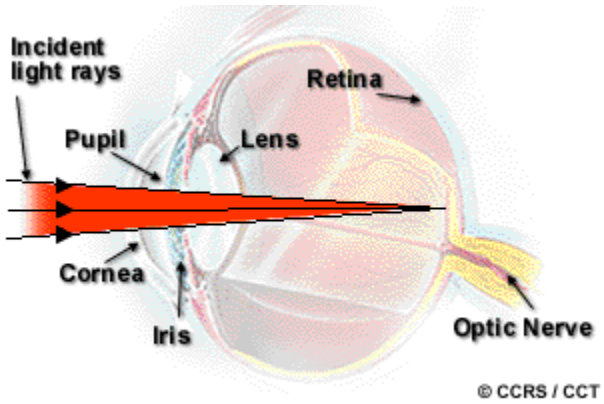

Having passed through the iris, light waves strike the lens. With its two curved surfaces, the lens further refracts light. Muscles in the eye control the focal length, determining the amount of refraction. Eyes that are too long or have too much refracting power cause images to be focused in front of the retina. This condition is known as near sightedness. Farsightedness occurs when the eye is too short or refracts too little causing images to be focused behind the retina. A perfect eye focuses light energy into an image on the retina.

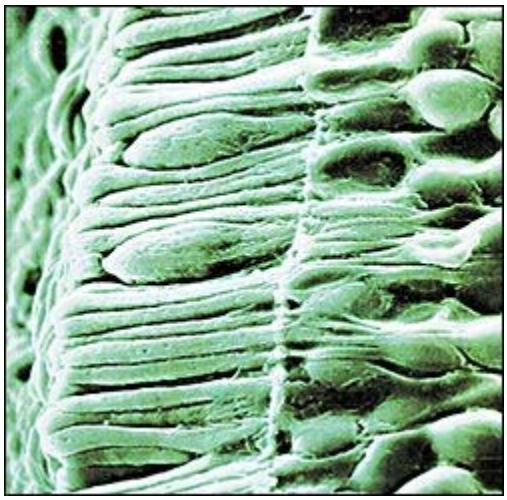

The retina is the inside lining of the rear surface of the eye. It contains cells that convert light energy into electrical impulses. These specialized light receptor cells are the **cones and rods**. Cones are highly concentrated in the central fovea, a small pit near the intersection with the optic nerve. They are used for detailed acuity in bright light and allow us to see colour. In contrast, rods are spread in the periphery of the retina, and are used in reduced light allowing us to see only black and white. The reception of light at the retina is the last passive stage in the vision process.

Having been converted to electrical impulses, light energy now travels through the axons of the cones and rods. The axons join together to compose the optic nerve. It carries the electrical stimulus to the brain stem, where receiver nerve cells connect with the optic

nerve cells. Signals from the stimulated receiver cells travel to the occipital lobe at the back of the brain where they connect with other brain cells to produce vision.

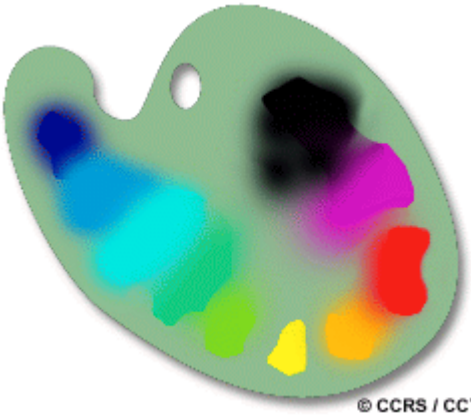

2.2.1 Colour Perception

In every day life, objects are described by particular **colours**, and often are identified with reference to familiar things. For example, as blue as the sky, as green as grass, as white as snow are common terms used to describe the colours. From the scientific perspective, the theory on the physics of colour began with Isaac Newton early in the 18th century. Using a **prism**, he separated sunlight into a spectrum of colours. He was able to distinguish seven colours: violet, indigo, blue, green, yellow, orange and red. Newton was able to separate rays of sunshine because light from different wavelengths is refracted by varying degrees when passing from one medium (air) to another (a crystal prism).

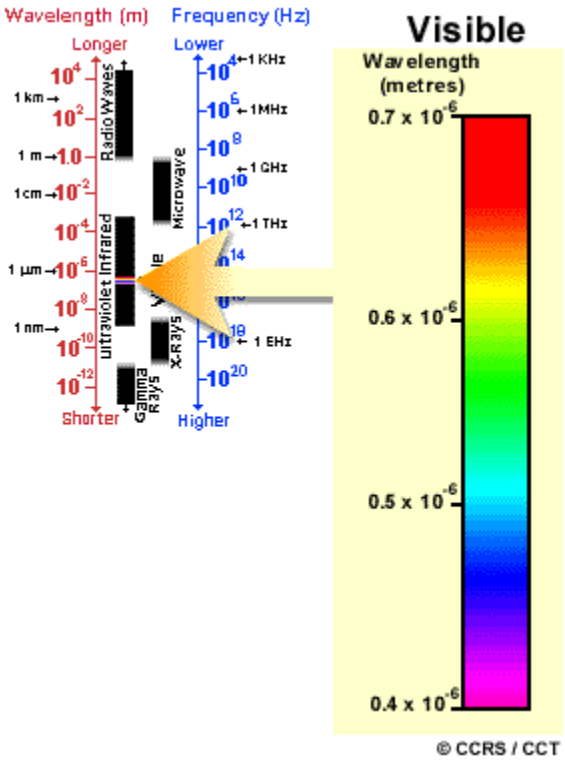

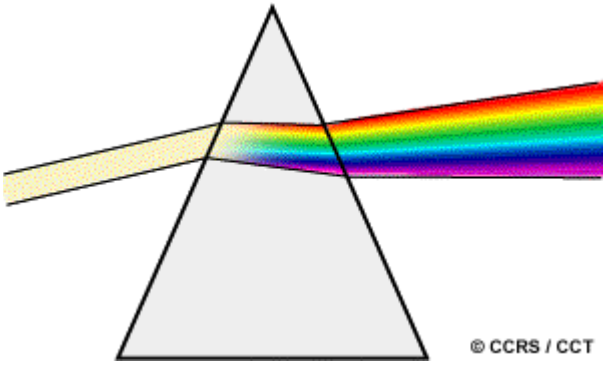

Wavelengths within the **visible spectrum** range from 400 to 700 nanometres. Within this spectrum an infinite number of colours can occur. A **colour can vary** in hue (chromaticity), intensity (brightness), or saturation (purity), separately, or in combination with the other components. It has been shown that with experience, humans can discriminate 120 or more hues when intensity and saturation are held constant. More, if intensity and saturation vary. However, with practical experiments scientists have shown that, most commonly, differentiation begins to break down when more than 7-12 colours along with black, white and grey tones are used at the same time in a display.

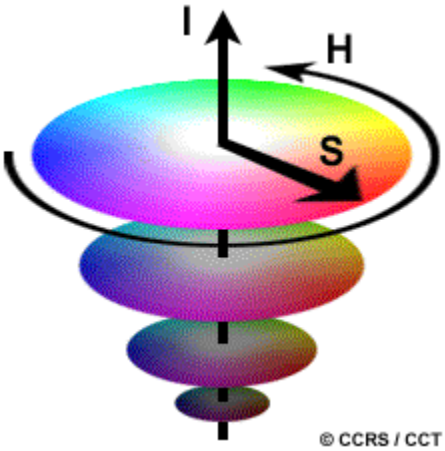

2.2.2 Depth Perception

Depth perception is based on 10 cues. These cues contain information which, when added to the 2-D image projected onto the retina, allow us to relate the objects of the image to 3-D space.

There are four physiological and six psychological cues.

The four physiological cues are:

1. accommodation, the adjustment of the focal length of the lens;
2. convergence, the angle made by the two viewing axes of a pair of eyes;
3. binocular disparity, the disparity between images of the same object projected onto the retinas; and
4. motion parallax, the result of changing positions of an object in space due to either the motion of the object, or of the viewer's head.

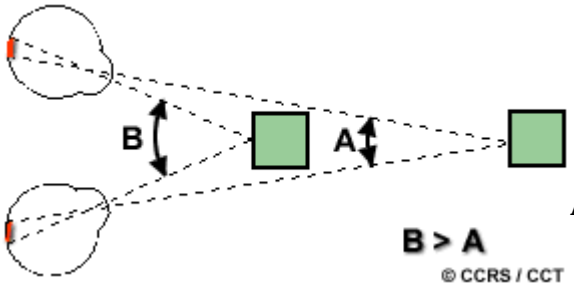

Accommodation & Convergence

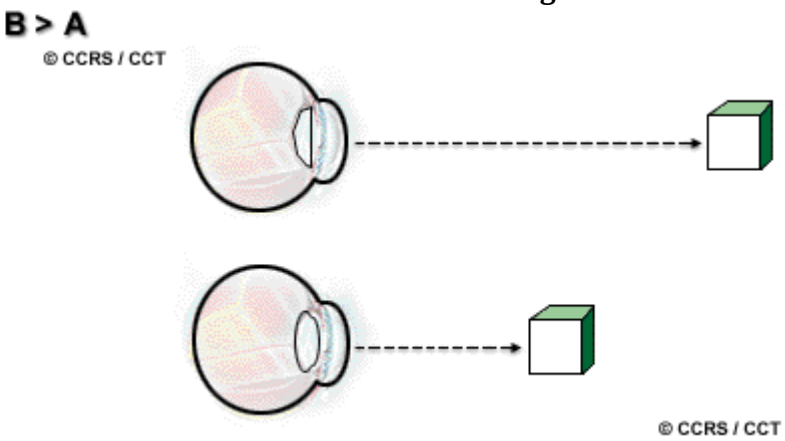

Accommodation and **convergence** are associated with the eye muscles, and interact with each other in depth perception. Accommodation is considered a monocular depth cue since it is available even when we see with a single eye. This cue is effective only when combined with other binocular cues, and for a viewing distance of less than two metres (Okoshi, 1976). Accommodation and convergence are considered to be minor cues in depth perception.

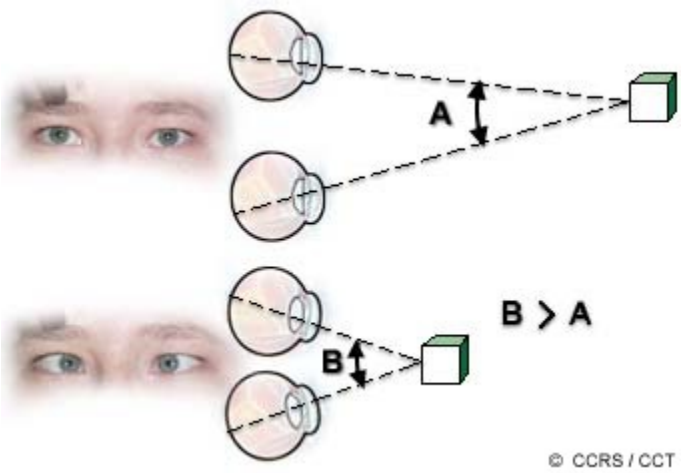

Binocular Disparity

Binocular disparity is considered the most important depth perception cue over medium viewing distances. Binocular parallax is the difference between the images of the same object projected onto each retina. The degree of disparity between the two images depends on the parallactic (convergence) angle. This is the angle formed by the optical axes of each eye converging on an object. The parallactic angle is related to the distance of an object from the eyes. At great distances the parallactic angle decreases and depth perception becomes increasingly difficult. The smallest parallactic angle the average person is able to discern, is three arc seconds.

Visual Motion Parallax

Visual **motion parallax** is a function of the rate at which the image of an object moves across the retina. Distant objects will appear slow in comparison with close objects even when the two are moving at the same speed. Motion parallax can also be caused by the movement of the viewer's head. Objects closest to the observer will appear to move faster than those further away. This is an important cue to those who only have the use of one eye.

The Six Psychological Cues

1. retinal image size, the larger an object image the closer it appears;

2. linear perspective, the gradual reduction of image size as distance from the object increases;

3. aerial perspective, the haziness of distant objects;

4. overlapping, the effect where continuous outlines appear closer to the observer;

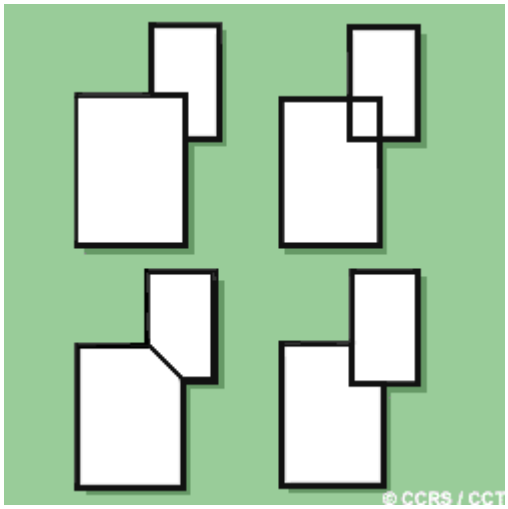

5. shade and shadows, the impression of convexity or concavity based on the fact that most illumination is from above; and

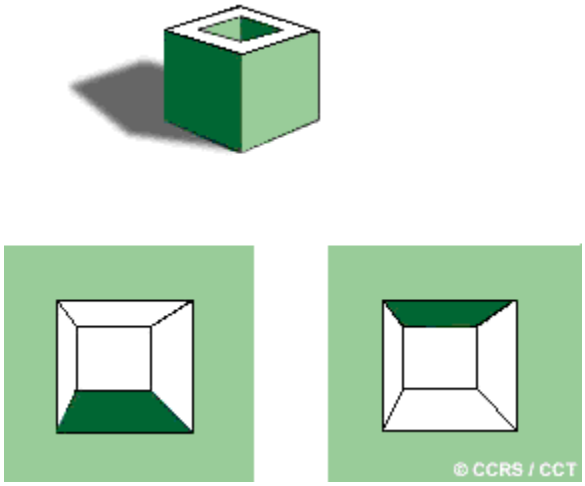

6. texture gradient, a kind of linear perspective describing levels of roughness of a uniform material as it recedes into the distance.

Psychological cues are learned cues, therefore, they are assisted by experience. **When combined**, these cues enhance depth perception greatly.

In remote sensing, several cues are used to represent depths of terrain. Perspective views of remotely sensed data, created with digital elevation models (DEM) and orthorectified images, provide an important source of 3-D visualization. When stereo viewing aerial photographs and other visible light imagery, such as that supplied by the Landsat, SPOT (Système pour l'observation de la Terre) or other satellites, binocular disparity is the most important cue.

Stereo viewing of radar imagery combines binocular disparity and shade and shadow cues for effective depth perception.

3. Viewing Methods in 3-D

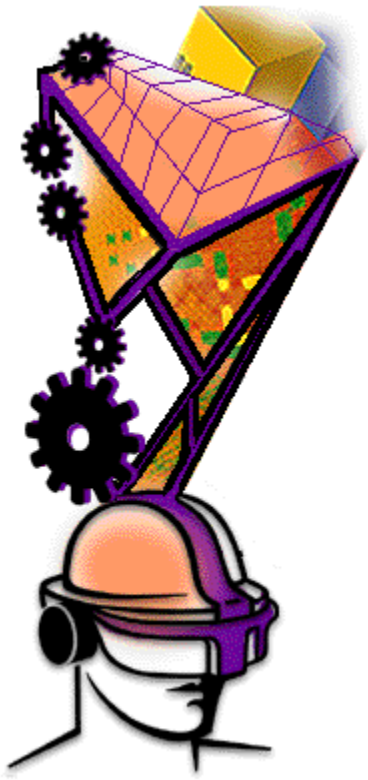

© CCRS / CCT

Since prehistoric times people have attempted to reproduce what they see naturally through drawing, painting and sculpture. In order to overcome the limitations of two-dimensional surfaces, psychological cues such as perspective, shade and shadows have traditionally been used to create an illusion of three-dimensionality. In the last 200 years, **mechanical-optical and digital 3-D imaging methods** capitalizing on the physiological cues of binocular parallax and convergence have been developed. Prior to the invention of holography, three-dimensional imaging techniques such as stereoscopy relied on these two cues. The following sections describe some commonly used 3-D imaging methods and systems, especially those related to remote sensing.

© CCRS / CCT

3.1 Stereoscopy

The first attempt to produce a stereoscopic image was undertaken by Giovanni Battista della Porta around the year 1600. More recently, artists such as Magritte in "Man with a Newspaper" (1928, The Tate Gallery, London) and Dali in "Christ of Gala" (1978, Museum Ludwig, Cologne) have created stereo-paintings by depicting left and right perspectives. **Drawing and painting techniques** were commonly used until the 1800's when they were rendered obsolete by the invention of photography.

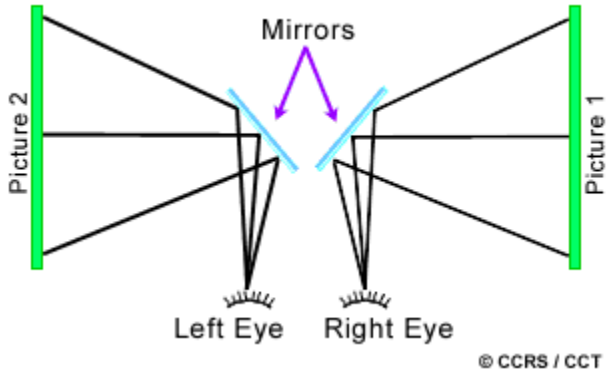

First stereoscopic viewer

The invention of photography in 1822 prompted the development of stereoscopes. The **first stereoscopic viewer**, a simple two-mirrored device, was proposed by Sir Charles Wheatstone in 1838. This simple device allowed a viewer to observe stereoscopic

pictures larger than the span that separates two human eyes, which is approximately 5.6 cm.

His idea was improved upon by Sir David Brewster who, in 1849, constructed a practical **stereoscope using prisms** instead of the mirrored model designed earlier.

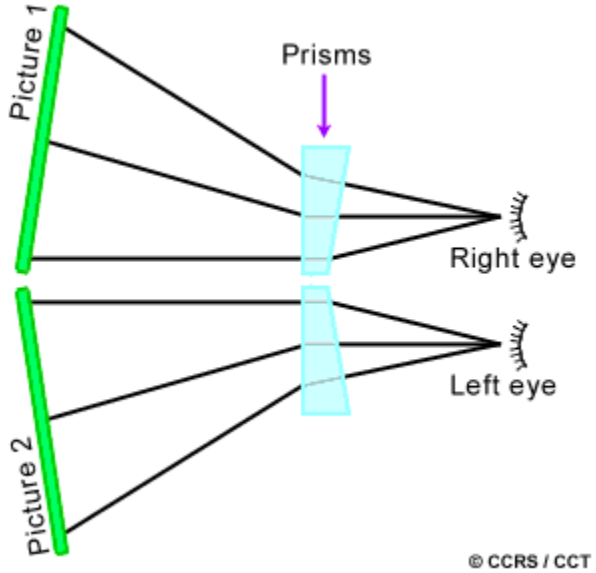

Stereoscope using prisms

Oliver Wendell Holmes improved the stereoscope by adding convex lenses as eyepieces (Okoshi, 1976). Such lenses improve depth perception greatly. When viewing a flat image, it is the "accommodation" cue which tells the observer that it is a flat picture. Adding a convex lens makes accommodation less significant. This allows depth sensation due to binocular parallax and convergence to be emphasized.

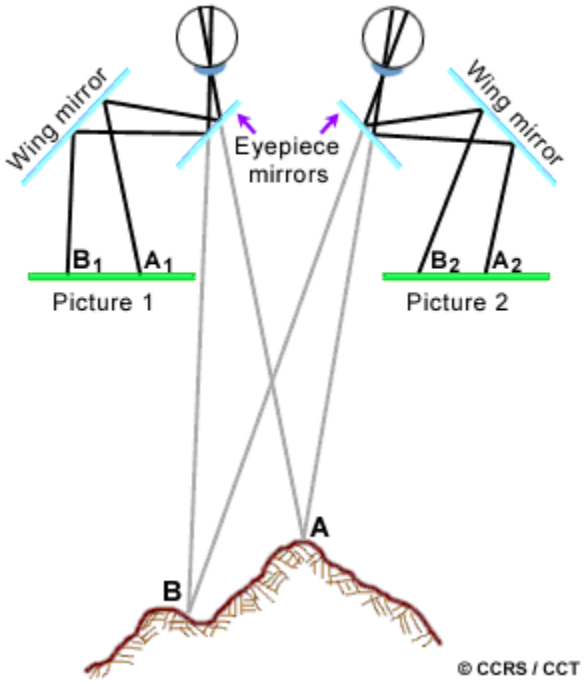

Stereoscopic viewing system

Stereoscopes allow us to see in three dimensions because they reinforce the physiological cues of "binocular parallax" and "convergence". A **stereoscopic viewing system** forces our eyes to see two images taken from different viewpoints at the same time. **Modern stereoscopes** range from relatively cheap pocket models that use only convex lenses, to more complex models that use mirrors, prisms and convex lenses.

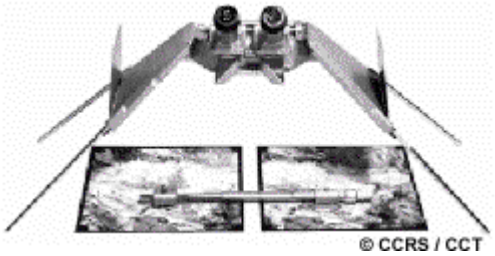

Modern stereoscopes

Cartographers, engineers, foresters, geologists, hydrologists and scientists from many other disciplines use stereoscopes. In order to increase their qualitative understanding of the environments they are researching, scientists use stereoscopes both in the field and in the office. Stereo viewing is also necessary for most mapping purposes.

Analogue stereoplotter

The last 40 years have seen the development of **stereoplotting systems**. The concept for these systems was developed in 1957 by U.V. Helava when he was employed at the National Research Council of Canada.

Photogrammetric principles - colinearity and coplanarity conditions - mathematically solve the relationship between image coordinates in a 2-D image reference system and the ground coordinates of objects in the 3-D 'real' world. The application of these mathematical concepts, in tandem with the development of computers, have allowed the generation of analytical and **digital stereoplotting systems**. The hardware and software used to transform information from 2-D digital imagery into 3-D data has allowed the mapping process to become increasingly automated. Reference material on analytical and digital stereoplotters can be found in such texts as the latest edition of the "Manual of Photogrammetry" published by the American Society on Photogrammetry and Remote Sensing.

Digital stereoplotter

Digital photogrammetric systems enable stereo viewing to be done on a computer screen using a system of optics and digital stereo images. Digital stereo images are separated

either spatially, radiometrically or temporally. Spatial separation is achieved by the use of two monitors or a split screen and an optical system using mirrors and/or convex lenses. Radiometric separation can be achieved by anaglyphic or polarization techniques and coloured or polarized lenses. **Temporal separation** is achieved by alternating the display of the two images.

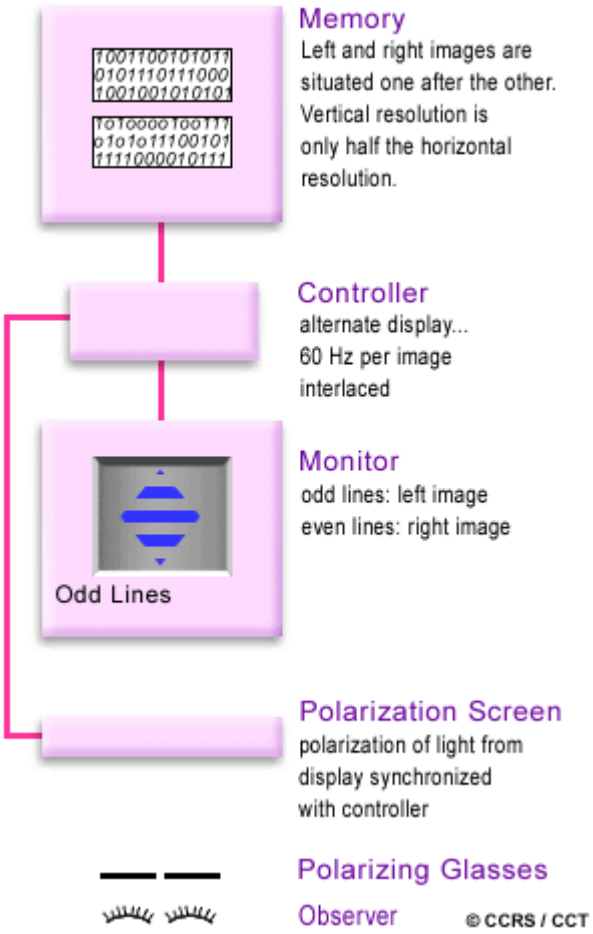

Temporal separation

Articles by Helava (1988), Dowman et al., (1992) and Heipke (1995) also present state of the art digital photogrammetric workstations.

3.2 Anaglyphs

Anaglyphic viewing systems also rely on parallax and convergence. Here, filters of complementary colours, usually red and blue or red and green, are used to separate left and right projections. The viewer wears a pair of glasses which cover the left eye with green (or blue) and the right with red. The left eye sees the overlap of the left image in green (or blue) while the right eye simultaneously sees the overlap area of the right image in red. This produces a three dimensional perception. Although inexpensive, this method has some inherent limitations. The source data is limited to black and white imagery. Colour imagery results in ghost effects on an anaglyphic image. Applying red and green

(or blue) filters to the original imagery causes light loss. This in turn causes some information to be lost. The red and green glasses may also cause eye fatigue.

Anaglyph image and glasses

3.3 Polarization

The use of light polarizing filters can also produce a 3-D effect. In this case, l projections are separated by polarized filters. This results in the two images h polarizations perpendicular to each other. Polaroid glasses are used to view th work in much the same way as the coloured anaglyphic glasses. By wearing t left eye sees the overlap area of the left image in one polarization while the ri simultaneously sees the right overlap area in a polarization at 90 degrees to th sensation of depth is produced. Polarization techniques cause very little light the use of colour imagery.

Digital Photogrammetric Workstation with a polarization screen and polarizing glasses

Film makers in the 1940s and 1950s employed both anaglyphic and polarization techniques to create **3-D mo** classics as "Swamp Monster from the Black Lagoon" and "It Came from Outer Space" were viewed wearing characteristic red and green and/or polarized glasses.

3.4 Chromostereoscopy

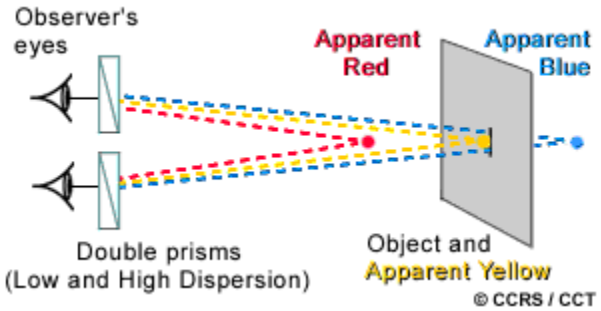

Chromostereopsis

Chromostereoscopy, or colour stereoscopy, is a three dimensional viewing system that does not rely entirely on binocular parallax and convergence. This method is based on the visual phenomenon of **chromostereopsis**. When chromostereopsis is positive, blue objects appear to be at a greater depth than red objects. Einthoven (1885) was the first scientist to study the chromostereopic effect. He attributed this effect to transverse

chromatic dispersion and the asymmetrical relation of the **visual and optical axes**. The visual and the optical axes of the eyes are not the same. Rays of light imaged on the fovea strike the corneal surface at an angle. As a result, the cornea and the two lens surfaces act as prisms. Shorter wavelengths (blue) are refracted more than longer wavelengths (red). On the retina, blue light is focused towards the nose while red light is focused towards the temples. Therefore, the red object will appear to be closer than the blue object.

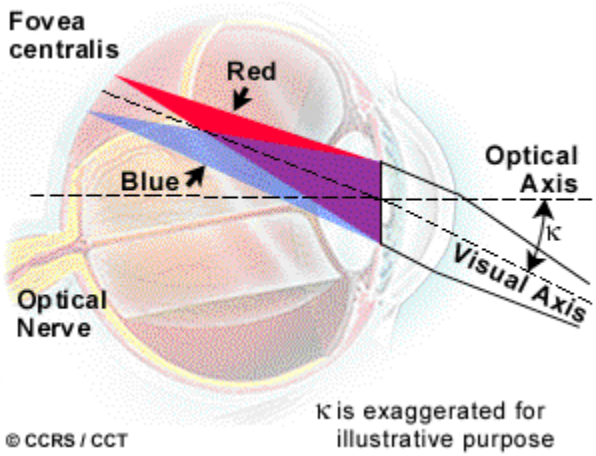

Visual and optical axes

Chromostereopsis can be enhanced by using principles of refraction (Newton, 1704). Light passing through a prism is **refracted** by an amount dependent on the wavelength of the light and the speed at which it travels through air and the glass of the prism. Using the principles of chromostereopsis, Richard Steenblik developed ChromaDepth^{TM} 3-D glasses in 1986. These glasses became commercially available in 1992. The lenses of these glasses are clear plastic, but act like thick glass prisms. They combine refraction and diffraction in a system of high precision micro-optics. The lenses shift image colours in different directions for each eye thereby creating a stereo perception from a single image.

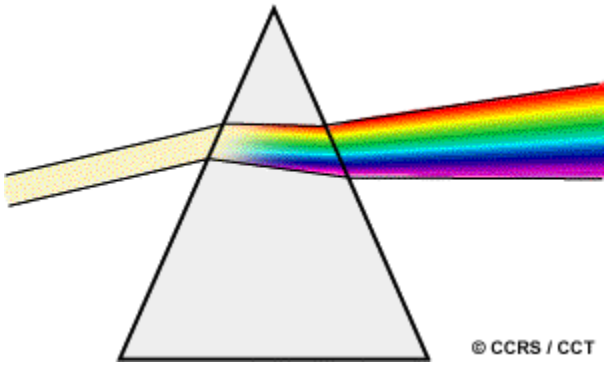

Prism

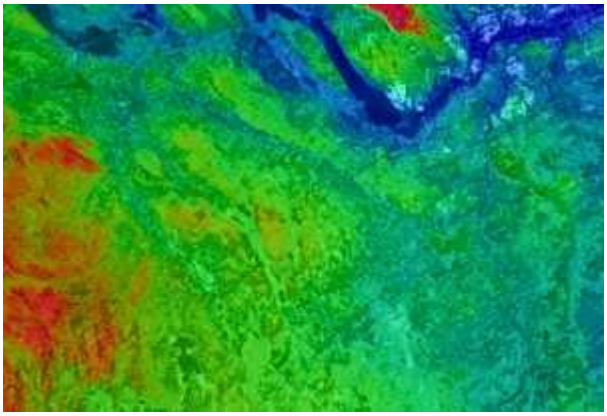

The method by which chromostereopsis can be used to create **3-D imagery** is to encode depth into an image by means of colour and then to decode the colour by means of optics such as the ChromaDepth™ glasses. In this way 3-D images can be created and presented in a variety of mediums including print, film, video and computer graphics. A 3-D display technique using the ChromaDepth™ glasses has been used to enhance **qualitative analysis** of remotely sensed data combined with geoscientific data (Toutin and Rivard, 1997).

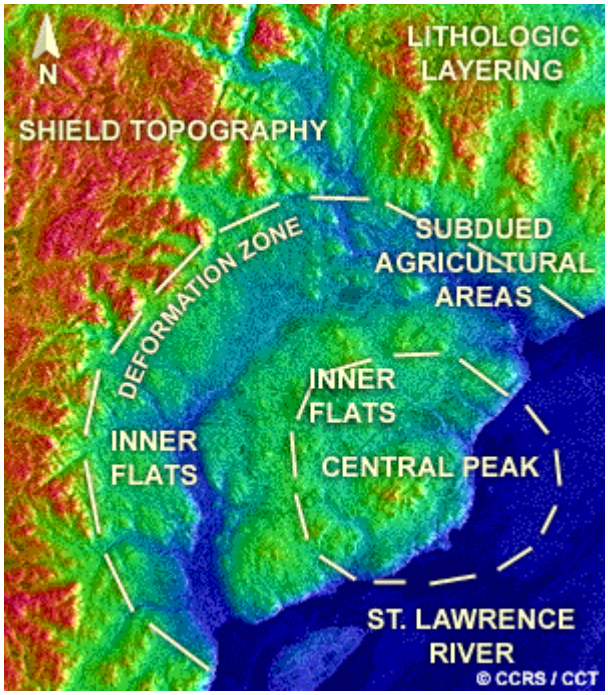

Qualitative analysis using 3-D display

3.5 Holography

Holography is the only true 3-D photography. It recreates the 3-D environment of light reflecting from an original scene. Just as the imaged object, holograms are viewable from any perspective. In theory, the original and the image should be indistinguishable. For example, if a hologram was made of a stamp under a magnifying glass, the stamps will

change as we change our viewing angles exactly as if we were viewing the real scene. The magnifying glass in the hologram magnifies the stamps as we change our point of view. However, technology has yet to catch up with theory. Researchers are continuing to develop ways in which to improve holograms.

Holography is an imaging technique, which uses wave properties of light and/or other energy to create 3-D images. The use of wave properties to create imagery was first proposed by Dennis Gabor (1948), who won a Nobel prize for his idea in 1971.

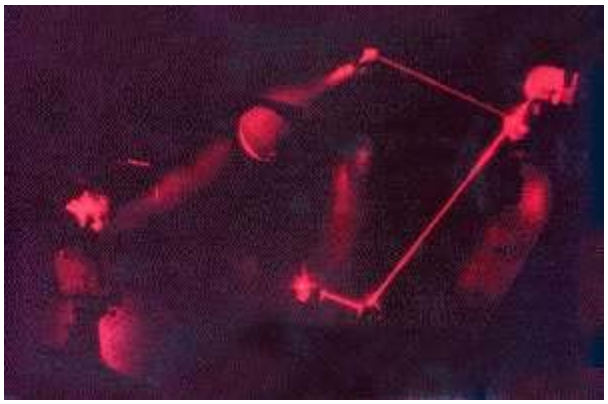

Creating holograms - First

Holography makes use of binocular parallax, convergence and accommodation cues (Friedhoff and Benzon, 1991). Holographic images can be viewed from as many different perspectives as the object being imaged. Two steps make up the holographic imaging process. **First**, the interference pattern containing information corresponding to both the wave amplitude and phase scattered by an object is **recorded** on a transparency to create the hologram. **Second**, the developed hologram is reconstructed.

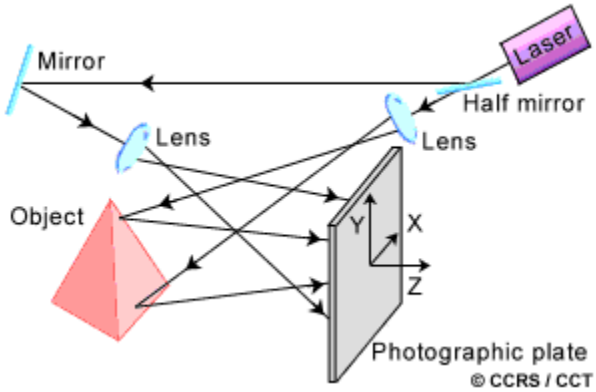

Creating holograms - Second

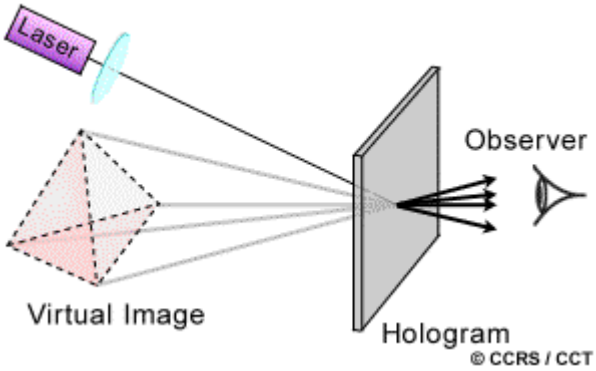

Creating holograms - First

Since the 1960s, researchers have progressed in overcoming disadvantages in the holographic imaging process. Some of the drawbacks of holography are:

- a darkroom is needed to record an object image;
- the object must be stationary;
- laser light illumination is dangerous to the human eye;
- ordinary holograms allow only for a black and white image to be created;
- recording of large objects is impractical because high powered lasers are not yet available;
- speckle noise and modulation noise are present;
- the reconstruction process is very inefficient;
- high-resolution photographic plate or film is very expensive; and
- a large amount of redundant information results from the recording process.

In short, holography is not yet an economical or easy process. Specialized recording and reconstructive devices are needed and an extremely well controlled environment is necessary. Techniques such as white light recording and reconstruction, colour holography, pulse laser beams, and reduced information holography are promising possible solutions to holographic imaging problems.

Holography has been applied to remotely sensed data (Benton et al., 1985). This group of researchers generated white-light viewable holographic stereograms using a digitally and optically processed Landsat MSS stereo pair. This resulted in a black and white 3-D image of the Earth's surface.

3.6 Other 3-D Imaging Methods

The search for more effective 3-D imaging methods continues. The following describes two recently developed methods which exploit the physiological cues of binocular parallax and convergence.

VISIDEP™ is a 3-D imaging technique invented in the early 1980s (McLaurin et. al. , 1988). This method employs a modified alternating-frame system that allows for a 3-D representation with vertical rather than a horizontal parallax.

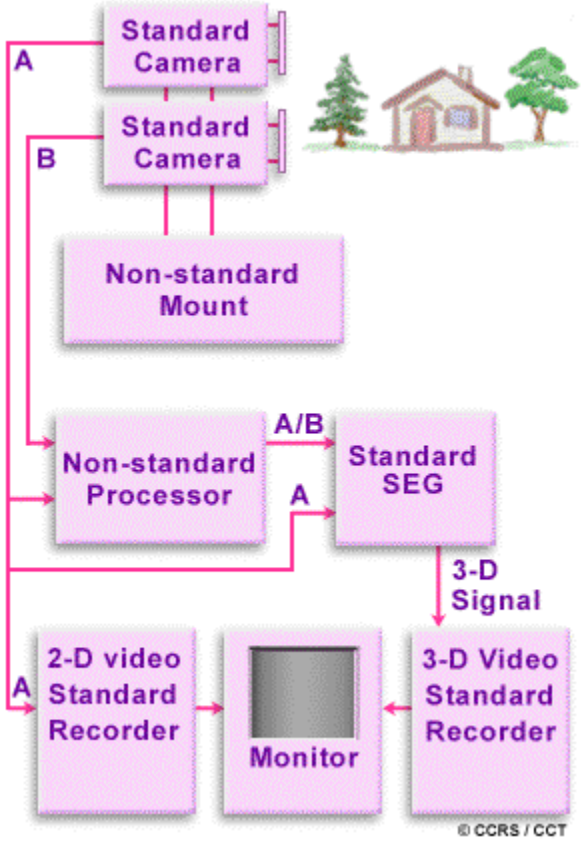

SEG = special effects generator that allows the mixing of two incoming channels into a single outgoing channel

Two cameras are used to generate images optically aligned on a vertical plane. A **single-source camera** in near-real time for three-dimensional imaging has also been mounted on a moving platform. This system has proven to be useful (Imsand, 1986) and adaptable to almost any situation with two sources of information (McLaurin et al., 1988). VISIDEP™ has been used for some remote sensing and geographic data applications (Ursery, 1993).

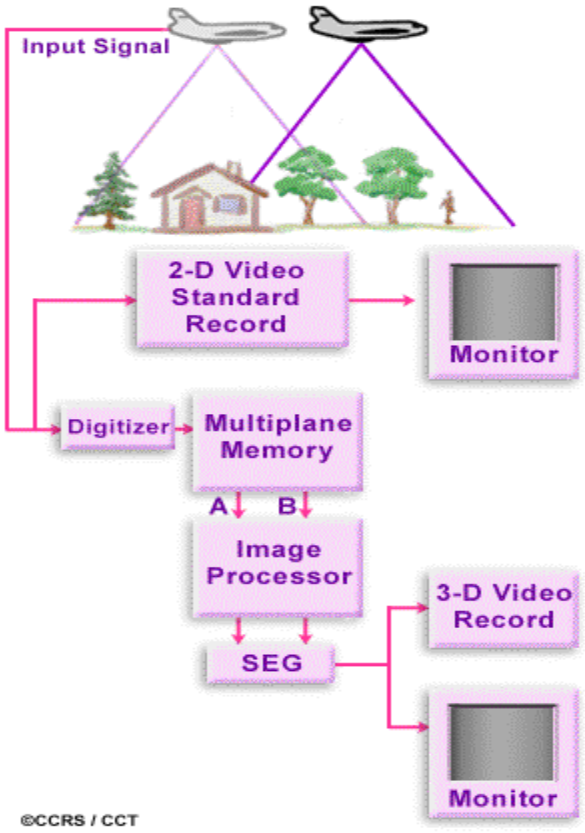

SEG = special effects generator that allows the mixing of two incoming channels into a single outgoing channel

Sharp Laboratory researchers in Europe (Photonics Spectra, 1995) have recently developed a **3-D moving image technology**. This is a prototype display system producing high-quality 3-D pictures based on two superimposed flat-screen panels. Twin liquid displays (LCDs) are placed at right angles, one horizontal and the other vertical. The images are combined by a proprietary optical filter, which transmits the image from one display, reflects the image from the other, and in doing so creates a 3-D image. A tiny silver spot is placed on the viewer's forehead so that the system can monitor the position of the viewer's head. This allows updates of the screen image in such a way that it always appears to be at a constant angle of 20 degrees from any direction. Therefore, the viewer can look around the object image without the image flipping.

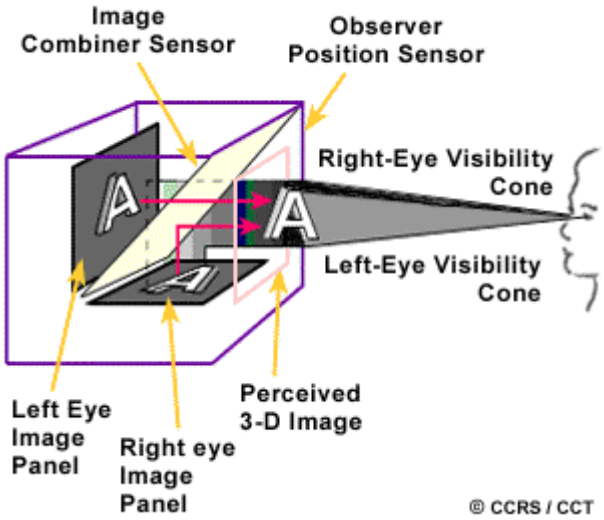

3-D moving image technology by Sharp Labs

4. Stereo Basics

Everything you wanted to know about stereo basics but were afraid to ask:

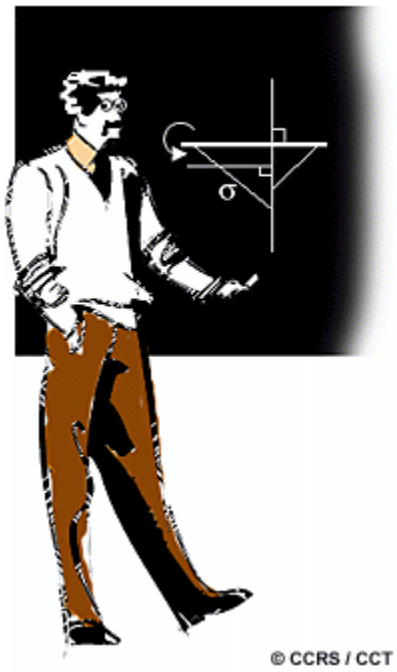

- How does stereo viewing work?
- What is Y parallax?
- What is vertical exaggeration?
- Why are two images better than one?

Read on and discover the answers in the following sections.

4.1 Stereo Viewing

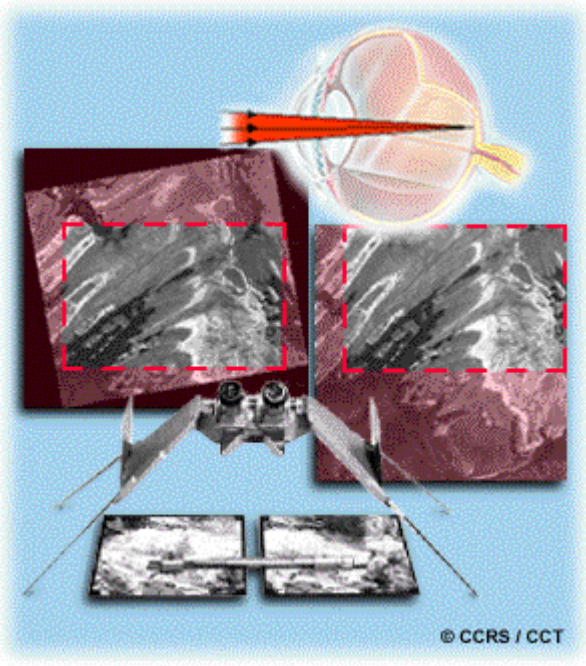

As mentioned in the previous section, **stereo viewing** reproduces the natural process of stereovision. Viewing a stereo pair of aerial photographs, satellite images, stereo paintings or any other kind of imagery is dependent on X parallax and parallactic angles.

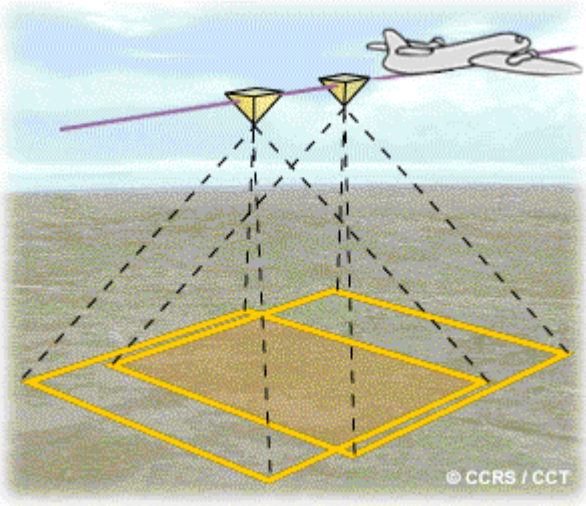

4.2 X Parallax

X parallax, which is also known as stereoscopic parallax, is caused by a shift in the position of observation. To **generate** a stereo pair of aerial photos, a camera on board an aircraft takes pictures of the Earth at different times and thus from different positions. Satellite image stereo pairs are generated when a satellite collects data with two different look angles or two different beam positions. The change in observation points causes an apparent shift in the position of an object with respect to the image frame of reference.

Two **fundamental aspects** of stereoscopic parallax are:

1. the parallax of any point is directly related to the elevation of that point; and

2. the parallax is greater for higher than lower elevations provided the viewing angle is constant.

These two relationships allow height measurements to be made from a stereo pair.

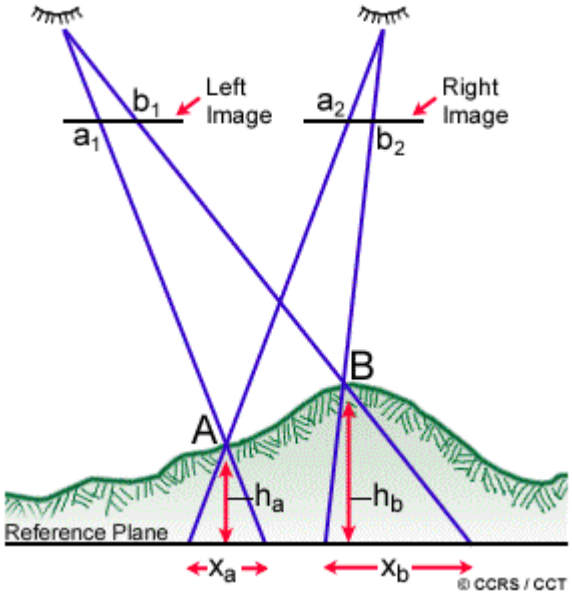

Stereoscopic paralax

- A = arbitrary point on the surface of the earth, at a lower elevation
- B = arbitrary point on the surface of the earth, at a higher elevation
- a_1, b_1 = points "A" and "B" as imaged on the left image
- a_2, b_2 = points "A" and "B" as imaged on the right image
- X_a = ground X-parallax due to the elevation of point "A" above the reference plane
- X_b = ground X-parallax due to the elevation of point "B" above the reference plane
- h_a = height of point "A" above the reference plane
- h_b = height of point "B" above the reference plane

4.3 Parallactic Angle

The **parallactic angle**, also known as the convergence angle, is formed by the intersection of the left eye's line of sight with that of the right eye. The closer this point of intersection is to the eyes, the larger the convergence angle. The brain perceives the height of an object by associating depth at its top and its base with the convergence angles formed by viewing the top and base.

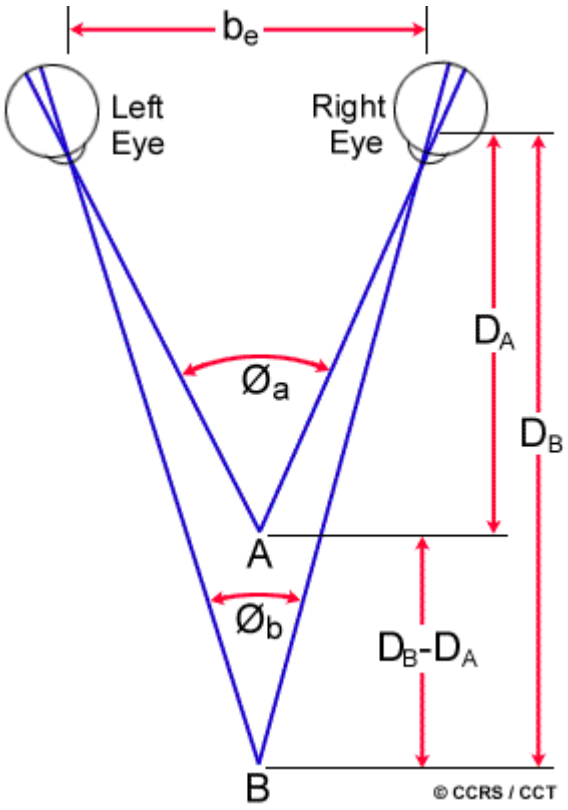

parallactic angle

- A = arbitrary point at higher elevation
- B = arbitrary point at lower elevation
- $Ø_a$ = larger convergence angle for higher elevation point
- $Ø_b$ = smaller convergence angle for lower elevation point
- D_A = apparent vertical distance to point "A"
- D_B = apparent vertical distance to point "B"
- D_B- D_A = difference in apparent vertical distances to points "A" and "B"

The X parallax and the parallactic angle are related. As X parallax increases, so too does the parallactic angle.

As the eyes scan overlapping areas between a stereo image pair, the brain receives a continuous 3-D impression of the ground. This is caused by the brain constantly perceiving the changing parallactic angles of an infinite number of image points making up the terrain. The perceived 'virtual' 3-D model is known as a stereomodel.

4.4 Y Parallax

Y parallax is present in many stereo pairs. It is the difference in perpendicular distances between two images of a point from the vertical plane which contains the air base. It can be caused by one or both images being **tilted** with respect to an exterior coordinate system. Tilt can occur as a result of roll, pitch and yaw of an aircraft. Y parallax can also

be caused by a **variation in flying heights**, or if images are printed at slightly different scales. Finally, Y parallax can occur if the viewer **lines up** the images incorrectly.

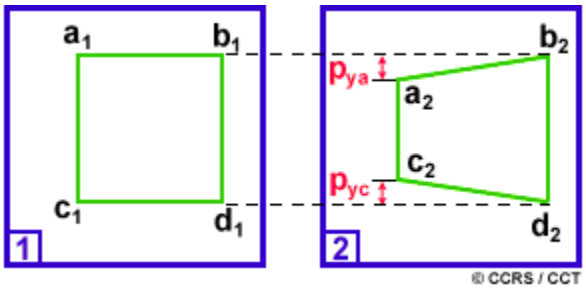

Y-Parallax due to tilt

- a_1, b_1, c_1, d_1, = arbitrary points on one image
- a_2, b_2, c_2, d_2, = corresponding points on other image with tilt
- P_{ya} = y-parallax of point "a" due to tilt
- P_{yc} = y-parallax of point "c" due to tilt

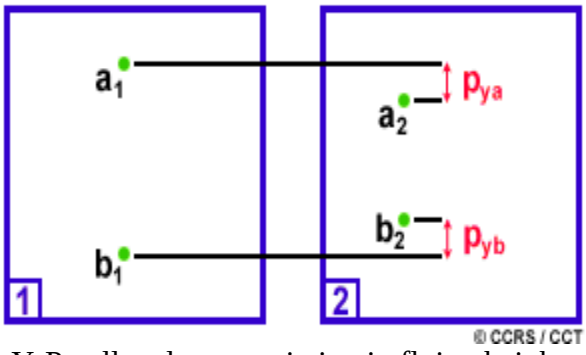

Y-Parallax due to variation in flying heights

- a_1, b_1 = arbitrary points on one image
- a_2, b_2 = corresponding points on other image with a scale difference
- P_{ya} = y-parallax of point "a" due to scale difference
- P_{yb} = y-parallax of point "b" due to scale difference

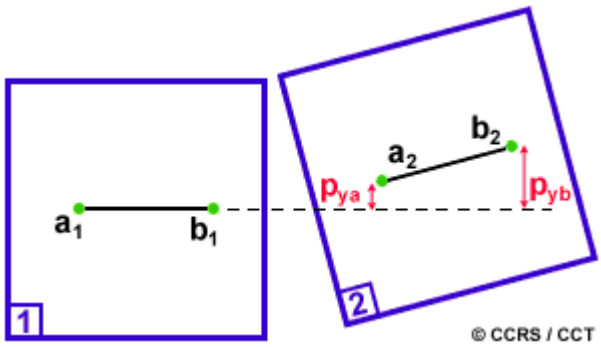

Y-Parallax due to mis-alignment

- a_1, b_1 = arbitrary points on one image
- a_2, b_2 = corresponding points on other image with a mis-alignment
- P_{ya} = y-parallax of point "a" due to mis-alignment
- P_{yb} = y-parallax of point "b" due to mis-alignment

In small amounts, Y parallax can cause eyestrain, however, the brain compensates and the 3-D stereo-model remains viewable. In large amounts, Y parallax makes stereo viewing of an image pair impossible. An example of a stereo image pair with too much Y parallax is given later.

4.5 Vertical Exaggeration

Vertical exaggeration is present in all stereo pairs. It exists because of disparity between the vertical and horizontal scales of a stereomodel. Under normal conditions, the vertical scale will appear greater than the horizontal. Image interpreters must take this effect into consideration when estimating heights of objects and rates of slopes.

Vertical exaggeration is best understood by considering the relationship between the **imaging geometry** and the **viewing geometry** of a stereo model.

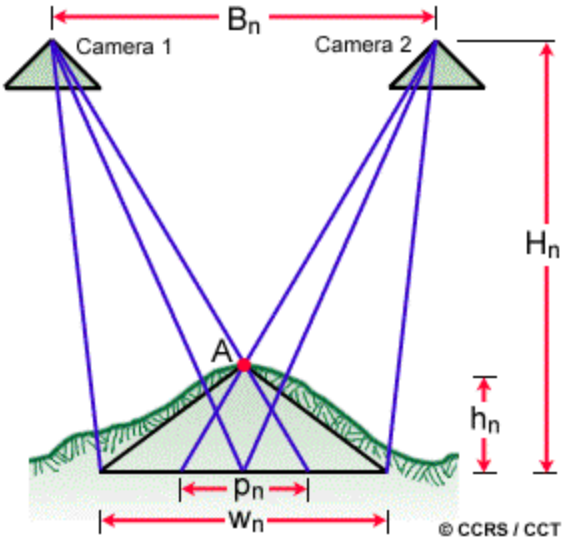

Vertical Exaggeration - Imaging Geometry

- B_n = air (imaging) base
- H_n = imaging height
- W_n = width of target
- p_n = parallax of point "A" due to elevation h_n
- h_n = target height

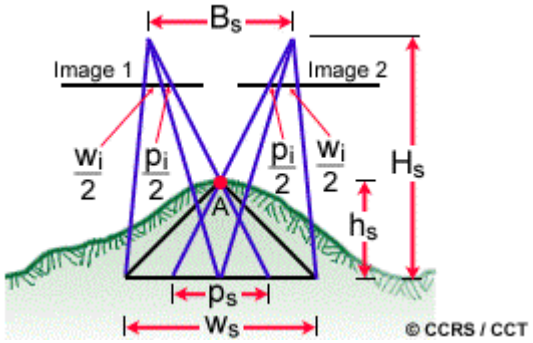

Vertical Exaggeration - Viewing Geometry

- B_s = stereo viewing base
- H_s = stereo viewing height
- W_s = apparent width of target
- h_s = apparent height of "A"
- p_s = apparent parallax of point "A"
- p_i /2 = one half of $p_s$as measured in one image
- w_i /2 = one half of $w_s$as measured in one image

Vertical exaggeration is the difference between the imaging base to height (B_n/H_n) and the stereo-viewing base to height (B_s/H_s) ratios. B_n/H_n is the ratio of the air base (distance

between the two exposure stations) to the flight altitude above average ground. B_s/H_s is the ratio of the eye base to the distance from the eyes at which the stereo-model is viewed.

4.6 Two Images - Not One!

Viewing imagery of the Earth's surface in stereo provides image interpreters with more qualitative and quantitative information than a single image. Cartographers, engineers, foresters, geologists, hydrologists and other scientists have traditionally used stereo viewing in their work. A stereo-model can convey information about slopes, shapes of landforms, and elevations much more clearly than a 2-D representation. Furthermore, stereo-models may show relationships between landforms and vegetation, mineral outcrops, or drainage systems that are not obvious from a single image.

A stereo pair also provides more quantitative information than a single image. This is important for mapping applications. In the monoscopic method, a single, two-dimensional image, with complementary data provided by a one-dimensional digital elevation model (DEM), can be rectified to generate an ortho-image. This is an image that is planimetrically correct, has an orthogonal projection, and can be superimposed on a map or other geocoded data. Like a map, X and Y cartographic coordinates can be extracted from ortho-images. However, they do not contain any height, or Z information, which can be obtained directly from the DEM. In contrast, with the stereoscopic method, a stereo pair can be directly used to extract the X, Y, and Z cartographic coordinates of ground features from the "virtual" stereo-model.

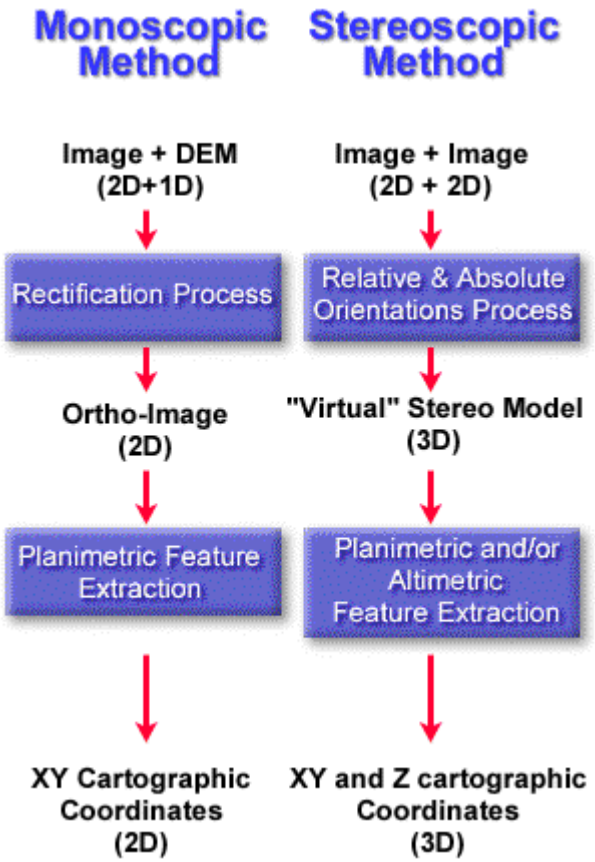

2D versus 3D viewing methods

Why can a stereo pair directly provide X, Y and Z coordinates? The answer is found in mathematics. Mathematically, an image is the representation of 3-D space in a 2-D medium. The physical constraint between the two spaces corresponds to the condition of collinearity well known in photogrammetry. This condition states that the exposure centre, the location of a ground point and its image point all lie on the same line. As a result of the collinearity condition, one degree of freedom is lost between 3-D reality and the 2-D image.

Consequently, extra information is necessary to reconstruct the third dimension from 2-D images. A single image can only give the row and line coordinates of image points. This is why terrain elevation information must be present in the ortho-rectification process. The 2-D single image added to the 1-D DEM gives us three pieces of information. In the case of a stereo pair, we have four pieces of information - two sets of row and line coordinates. Consequently, a stereo pair provides supplementary information for extracting the three X, Y and Z coordinates.

The ortho-image rectification process (monoscopic method) is dependent on the accuracy of the DEM. Errors in the DEM will propagate through ortho-image generation and feature extraction processes. As a result, planimetric features extracted from the ortho-image could be less accurate than those extracted from the stereo-model. In the stereoscopic method, planimetric feature extraction is independent of the altimetry.

Another advantage of stereo viewing is that it can be done directly from raw images. Resampling, which can degrade image radiometry and geometry thereby reducing interpretability, is unnecessary. On the other hand, resampling is part of ortho-image generation, adding another source of error to the process.

It has been proven that the ability to identify certain features in mono images is more difficult than in stereo. In thematic applications, stereo display gives a clear perception of terrain to better locate features such as control points, forest cover, clear cuts, river and stream beds.

5. Radar Basics

Radar is an acronym for RAdio Detection And Ranging. Radar systems were originally developed in order to detect the presence and position of objects using transmitted and received radio waves. Due to the electromagnetic properties of radio waves radar systems are capable of collecting data in nearly all atmospheric conditions, by day and/or night. For this reason they have proven to be useful in a number of applications.

Radar systems were first implemented in the 1930s to detect ships on water and to measure their proximity. Imaging radar systems have been in use since the 1950s. They were originally developed by the military. Radar as a remote sensing tool became more commonly used as military systems were declassified and scientists developed new applications in mapping and resource monitoring.

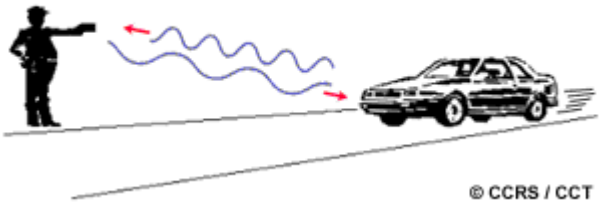

5.1 Imaging and Non-Imaging Systems

Radar systems may or may not be imaging systems. A well known example of a non-imaging system is a doppler radar system. These systems are used (for example) to **measure vehicle speeds** by measuring the frequency, or doppler shift between transmitted and return signals.

Plan position indicators (PPI) produce a type of image. These radars use a circular display screen to indicate objects surrounding the rotating antenna. They are commonly used for weather monitoring, air traffic control and navigational systems. The spatial resolution of the view map of the area under surveillance is too coarse to be used in remote sensing applications.

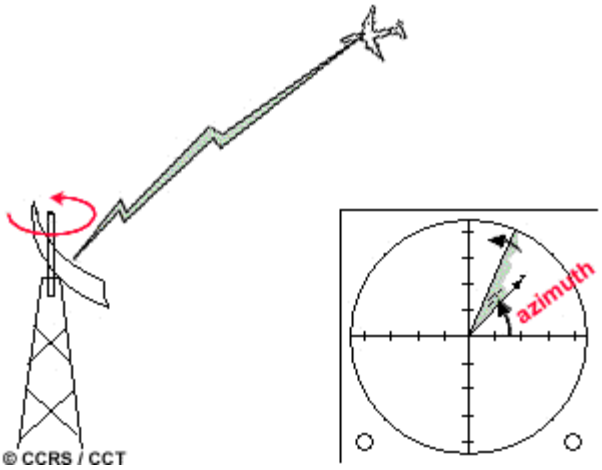

Radar imaging systems used in remote sensing applications consist of an **air** or space borne antenna. These antennas transmit and/or receive radar signals in order to produce imagery at a fine enough resolution for image interpreters to identify physical features on the Earth's surface.

Black bulge under fuselage (radome)covers the radar antenna.

5.2 Active and Passive Imaging Systems

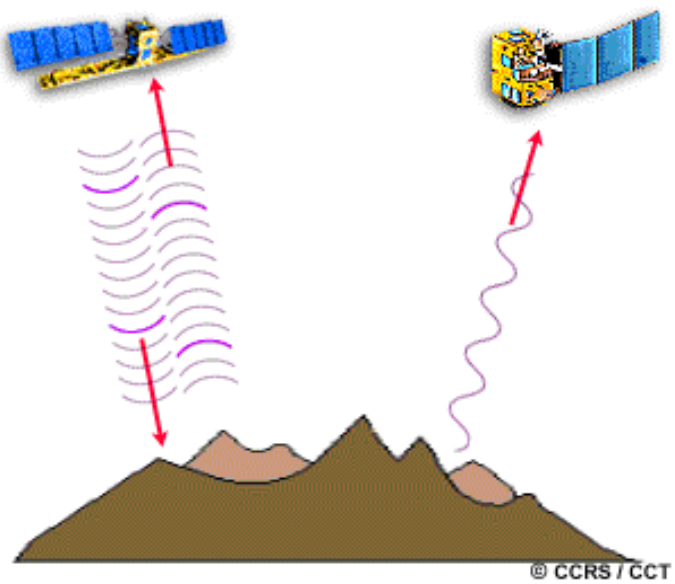

Active and Passive Radar Imaging Systems

Imaging radar systems can be active or passive. Active radar systems transmit short bursts or 'pulses' of electromagnetic energy in the direction of interest and record the origin and strength of the backscatter received from objects within the system's field of view. Passive radar systems sense low level microwave radiation given off by all objects in the natural environment.

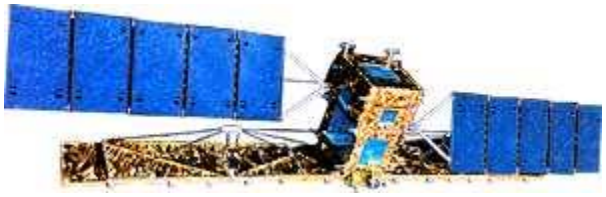

Radar imaging systems such as ERS (European Remote Sensing Satellite), JERS (Japan Earth Resources Satellite), and **RADARSAT-1** are active systems. They both transmit and receive energy. Microwave scanning radiometers only receive microwave energy. The Japanese **MOS** (Marine Observation Satellite) and JERS satellite systems employ microwave scanning units. Since the source is a very low level of electromagnetic energy, this type of data is prone to noise.

One advantage of active radar sensing systems is that, since they provide their own source of energy, they can collect data at any time of the day or night. Passive sensors - optical, thermal, and microwave - rely on receiving the naturally emitted or the sun's reflected energy from the Earth's surface.

5.3 Radar and the Electromagnetic Spectrum

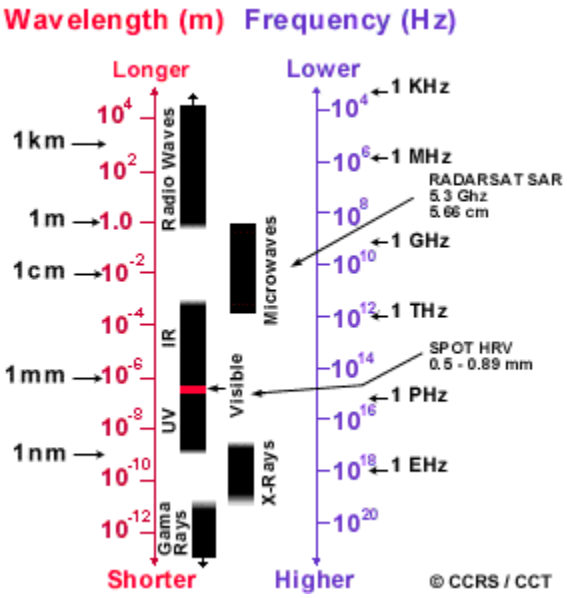

The electromagnetic spectrum

Radio waves are one component of the **electromagnetic spectrum** (EM). This spectrum describes wavelengths and frequencies of energy. Ultraviolet, visible light, x-rays, microwaves and thermal energy are other examples of electromagnetic energy. **The visible part of the EM spectrum** contains blue, green and red light with wavelengths in the range of 400 to 700 nanometres. **Infrared energy** ranges from 700 to more than 100,000 nanometres. **Microwaves** are much longer, ranging from 1 mm to 1 metre. The longest microwave is approximately 2,500,000 times as large as the smallest visible light wave. Radar band designations range from the Ka band occurring between 7.5 and 11.0 mm to the P band range between 30 and 100 cm.

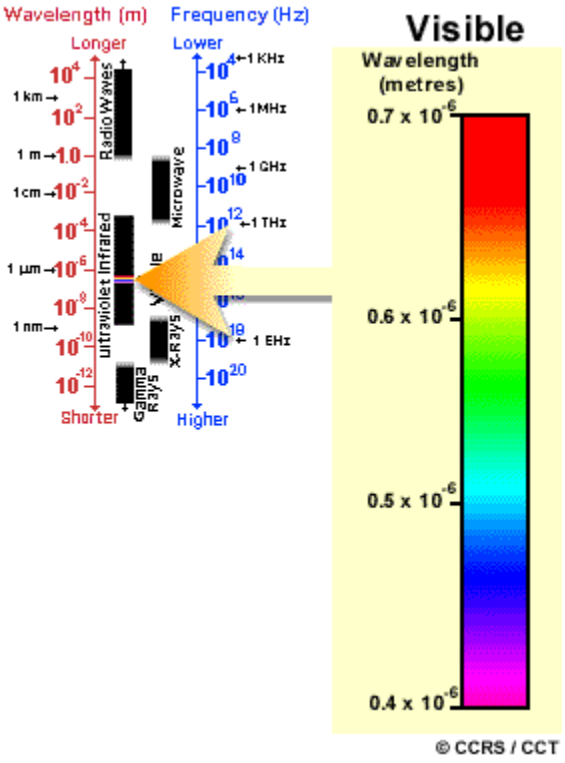
Wavelength (m)
Frequency (Hz)
Longer
Shorter
Lower
Higher
Radio Waves
Microwave
Infrared
Ultraviolet
X-Rays
Gamma Rays
1 km
1 m
1 cm
1 µm
1 nm
1 KHz
1 MHz
1 GHz
1 THz
1 EHz
Visible
Wavelength (metres)
0.7 x 10-6
0.6 x 10-6
0.5 x 10-6
0.4 x 10-6
© CCRS / CCT

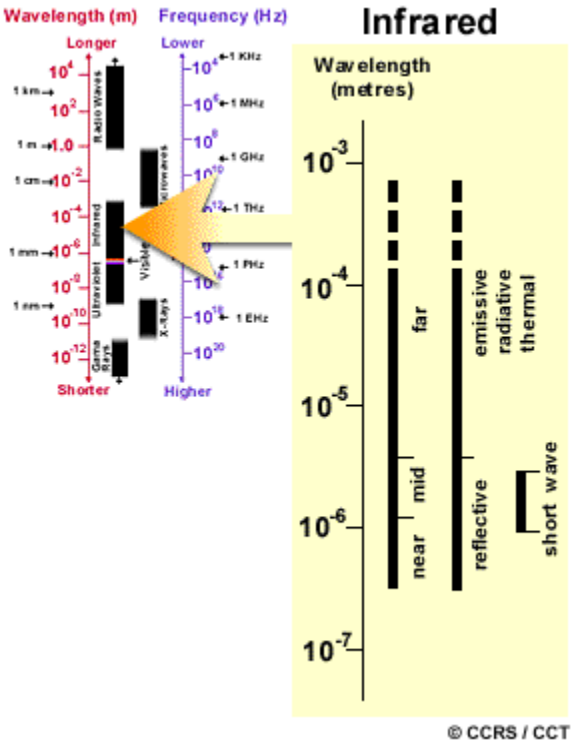
Wavelength (m)
Frequency (Hz)
Longer
Shorter
Lower
Higher
Infrared
Wavelength (metres)
10-3
10-4
10-5
10-6
10-7
far
mid
near
emissive
radiative
thermal
reflective
short wave
© CCRS / CCT

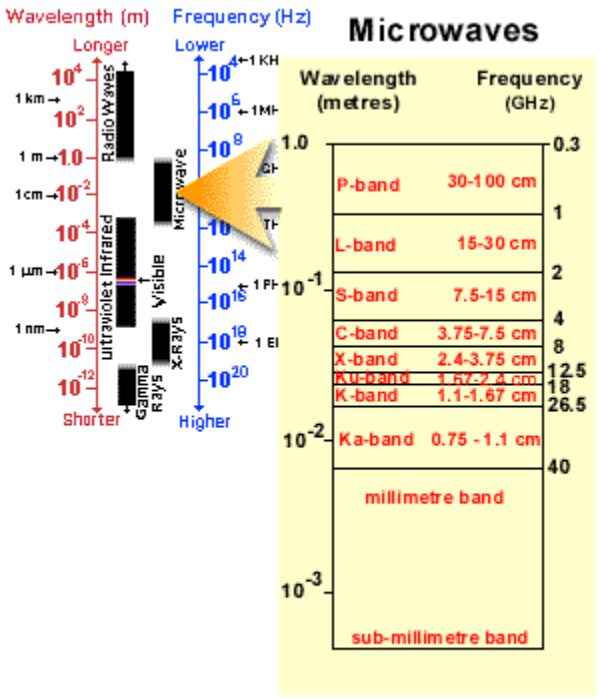

Any system transmitting and/or receiving energy from the Earth's surface is **affected by the atmosphere**. Water vapor, dust, smoke, airborne pollutants and other small particles close in magnitude to visible and infrared (VIR) wavelengths cause interference in the path between target and sensor. VIR wavelengths can be dispersed or blocked before they reach the sensors. Since microwaves are longer, they are not as affected by these types of small particle matter. Therefore, sensors transmitting and/or receiving microwaves are able to 'see' through haze, cloud, light rain, snow, smoke, and pollution. As a result, radar images can yield valuable information that is not available in VIR images.

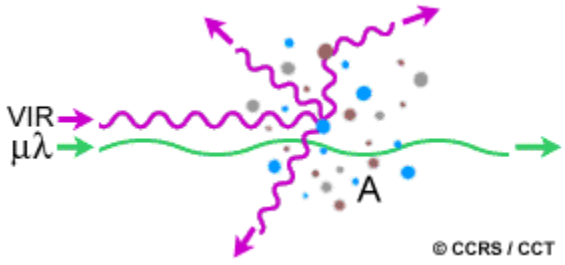

Atmospheric Penetration

- VIR = visible and near infrared radiation
- $\mu\lambda$= microwave radiation
- A = particles in the atmosphere (water vapour, dust, smoke, etc.)

5.4 Radar Systems in Remote Sensing

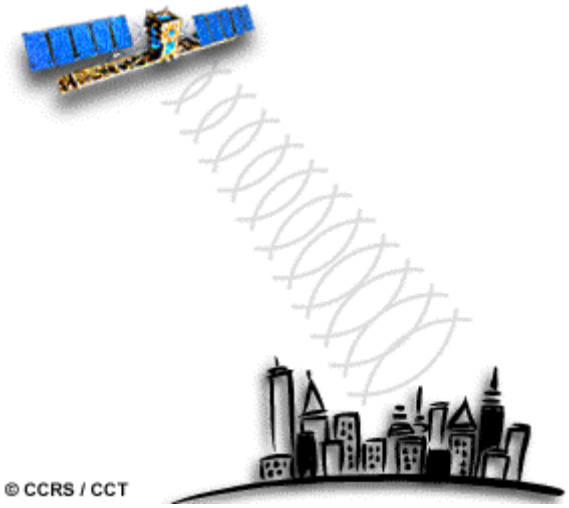

Radar Systems in Remote Sensing

In order to understand how a **radar imaging system** produces imagery, a comparison with optical imaging systems is useful. Photographs or scanned images are the product of systems which use visible light and near infrared radiation and are the result of near instantaneous exposure. In contrast, radar imagery is produced by recording microwave pulses travelling to and from a target area over a period of time.

The optics-equivalent in a radar imaging system is a long, rectangular antenna which transmits and receives microwave energy. Resolution, which is the ability of a system to differentiate between two closely spaced objects, is dependent on focal length in optical sensors and in the along-track direction antenna length in radar systems. Antennas are analogous to lens systems in that a long antenna can be compared to a telephoto (long focal length) lens, while a shorter antenna is similar to a wide angled (short focal length) lens. To continue the analogy, a long antenna provides a detailed, or high-resolution image of a small area, while a short antenna provides an image of a large area with less detail.

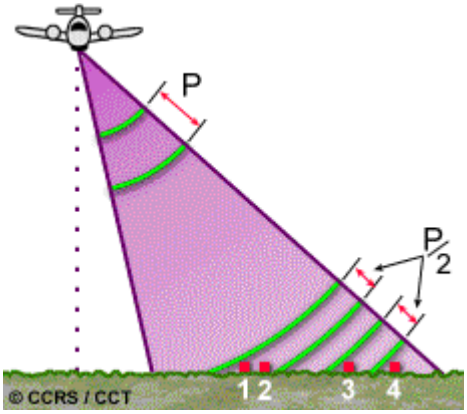

Range Resolution

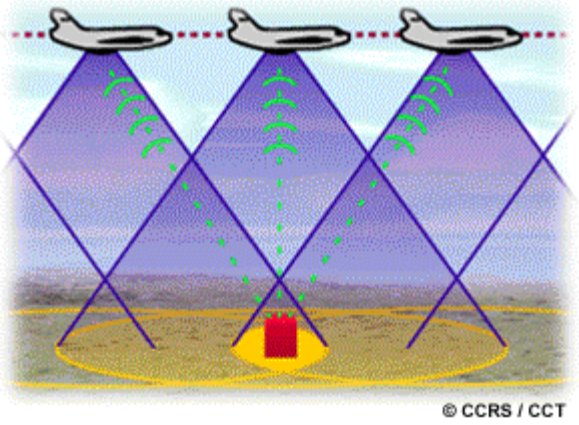

- P = pulse length
- 1, 2 = two targets that are too close together to be resolved as individual targets
- 3, 4 = two targets with sufficient range separation to be resolved as individual targets

Resolution in a radar system is controlled by the signal pulse length and the antenna beam width. The signal pulse length dictates resolution in the direction of energy propagation. This is referred to as the range direction. Shorter pulses result in a higher **range resolution**. The width of the antenna beam determines the **resolution in the flight or azimuth direction**. The beamwidth is directly proportional to radar wavelength and is inversely proportional to the length of the transmitting antenna. This means that resolution deteriorates with distance from the antenna. In order to have a high resolution in the azimuth direction the radar antenna must be very long.

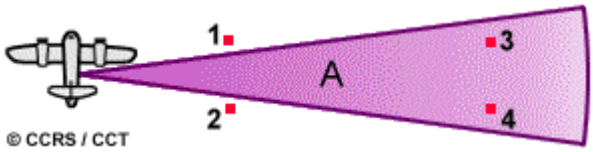

Resolution in the flight or azimuth direction

- A = antenna beam
- 1, 2, = two targets that can be resolved as being separate
- 3, 4, = two targets that cannot be resolved as being separate

Remote sensing radars can be divided into two categories - real aperture and **synthetic aperture radars** (SAR). Real aperture radars transmit and receive microwave signals with a fixed length antenna. They are limited in their ability to produce resolutions fine enough for most remote sensing applications, simply because it is difficult to transport a very long antenna. To solve this problem synthetic aperture radars (SAR) were developed. SARs have physically shorter antennas, which simulate or synthesize very long antennas. This is accomplished through modified data recording and signal processing techniques.

5.5 Imaging Geometry

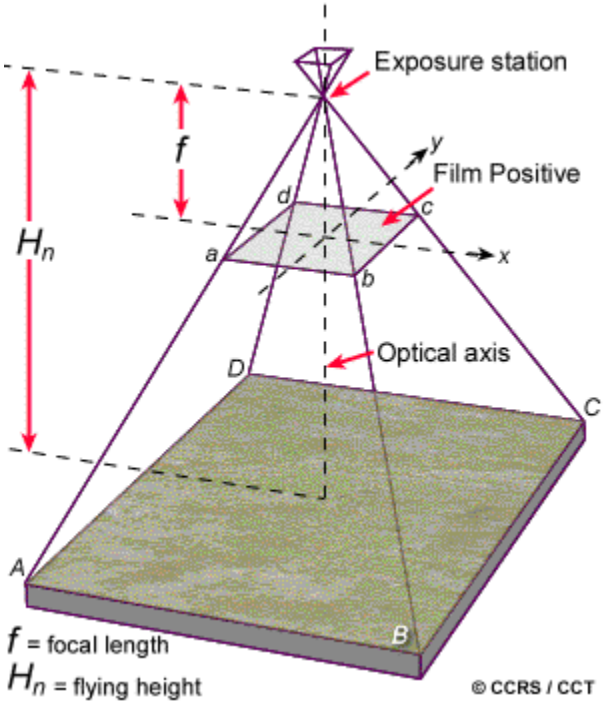

Photographic system geometry

The geometry of radar imaging systems and photographic systems or VIR imaging scanners is very different. Where **photographic systems** and most **scanners** employ a central, downward looking sensor and symmetrical geometry, **radar imaging systems** are characterized by a side looking sensor and asymmetrical geometry.

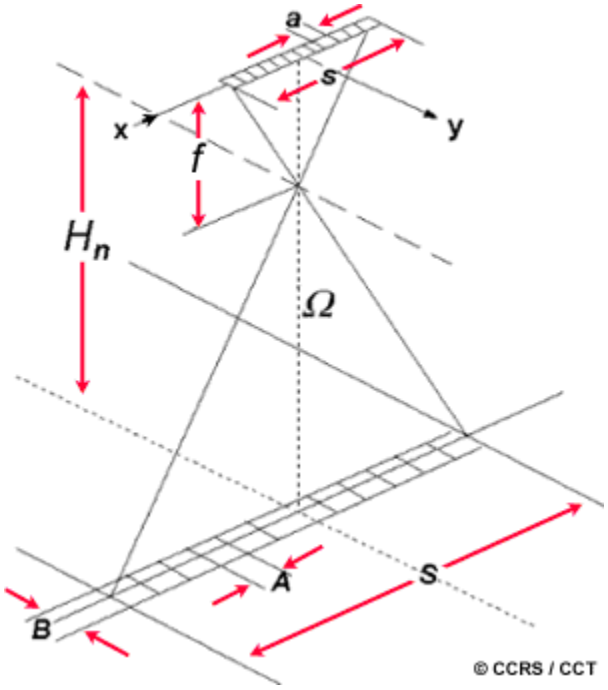

Scanning system geometry

- H_n = flying height
- Ω= field of view
- f = focal length
- a = size of detector element
- s = length of detector array
- S = length of scan line
- A = resolution in x direction
    - B = resolution in y direction

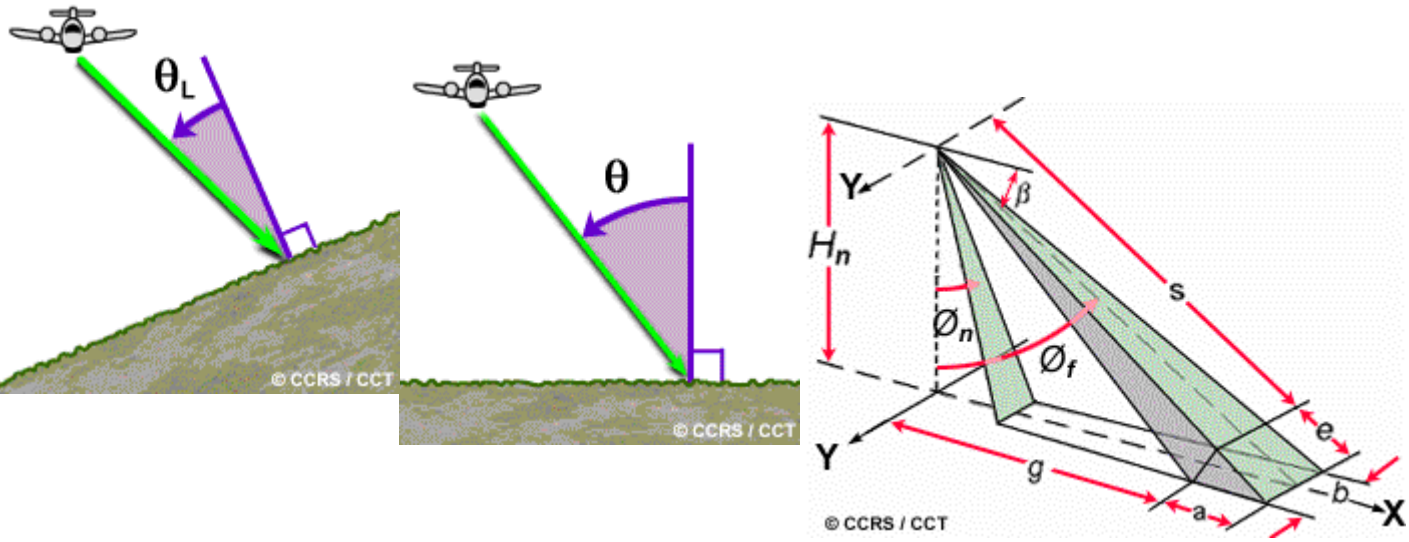

Radar system geometry

- H_n = flying height
- ß = depression angle
- $Ø_n$ = near edge incidence angle
- $Ø_f$ = far edge incidence angle
- s = slant range
- g = ground range
- a = ground range resolution (x direction)
- b = azimuth resolution (y direction)
- e = slant range resolution

5.6 Incidence Angle

Incidence angle describes the relationship between radar illumination and the ground surface. Specifically, it is the angle between the radar beam and a target object. The incidence angle helps to determine the appearance of a target on an image.

A **local incidence angle** can be determined for any pixel on an image. Trees, rocks, buildings, other structures and different terrains create changes in the local incidence angle. This in turn causes **variations in pixel brightness**.

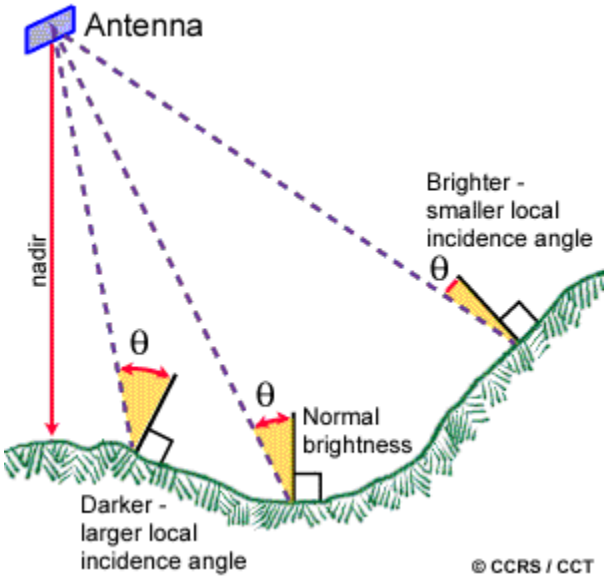

Local incidence angle influence on pixel brightness

Due to their greater altitude, satellite **incidence angles** vary less than airborne incidence angles. This leads to more uniform illumination on satellite images than airborne radar images.

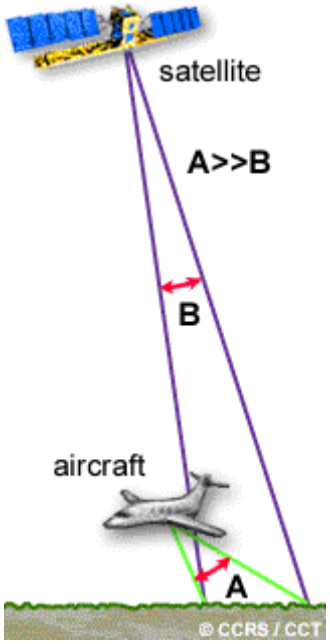

Incidence angle variation from aircraft versus satellites

5.7 Slant Range and Ground Range

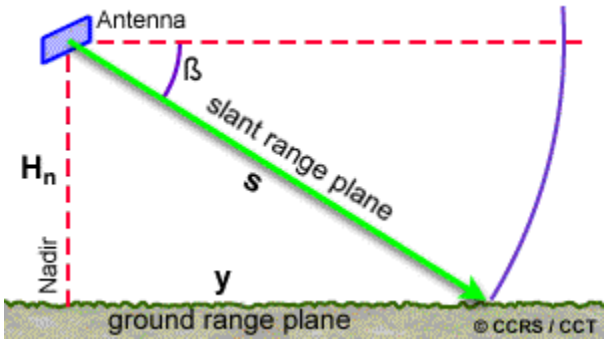

H_n = flying height ß = depression angle

Slant Range and Ground Range

Slant Range Image

Ground Range Image

Radar imaging systems record the differences in travelling times between return signals. The distance between an object and the antenna is equal to the speed of propagation of the wavelength through the atmosphere multiplied by the time it takes to reach the antenna. This, of course, is the relationship between the speed of EM radiation, time taken and distance travelled. A **direct relationship between the slant range and the ground range** also exists. Since we know the angles at which the microwaves are propagated, we can use trigonometry to **calculate the ground range**.

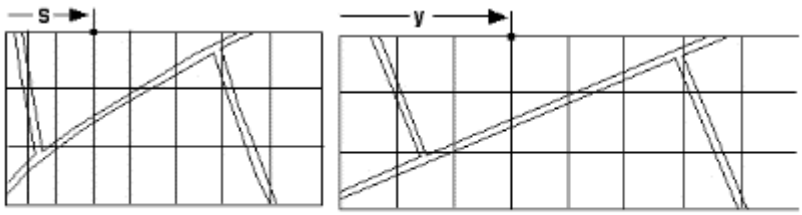

$s = (y^2 + H_n^2)^{1/2}$ $y = (s^2 - H_n^2)^{1/2}$ $\frac{y}{s} = \cos\beta$

In order to view a radar image in the more recognizable ground range configuration, a **geometric correction** between the two distances is made.

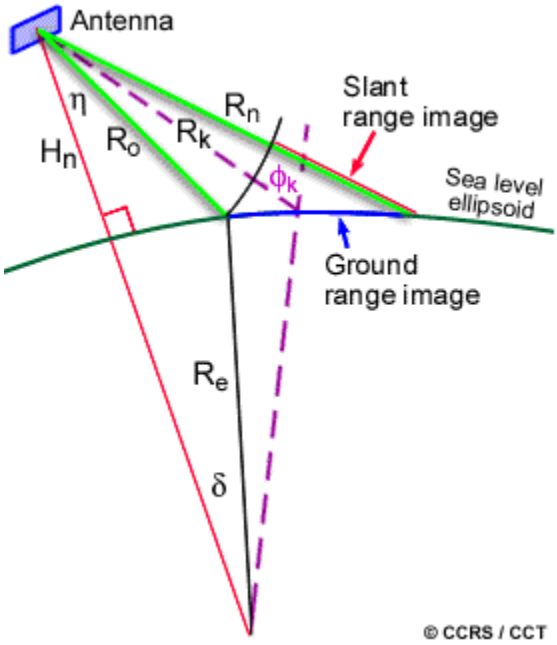

Geometric correction

R_o, ..., R_k, ..., R_n = slant range (km)
H_n = satellite altitude (km)
η= illumination angle
δ= Earth centre angle

$$\phi_k = \text{incidence angle}$$
$$= \arccos\left[\frac{(H_n^2 - R_k^2 + 2R_eH_n)}{2R_kR_e}\right]$$

The slant range to ground range distortion is much more pronounced in airborne SAR systems than it is in satellite SAR systems. This is a result of the difference in depression angles and the range of the depression angles between airborne and spaceborne SARs. The slant range to ground range correction may not be necessary in order to create an effective stereo pair from satellite SAR imagery.

5.8 Radar Imagery Versus VIR Imagery

How does radar imagery differ from VIR imagery?

A quick glance **comparing radar imagery with aerial photography or VIR satellite imagery** will reveal obvious differences. Imaging geometry and electromagnetic wave properties together produce the very different appearances of a radar image, an aerial photograph or a VIR satellite image. The following sections demonstrate the effects of imaging geometry and microwave properties on a typical radar image.

VIR image (left) and radar image (right) comparing radar imagery with aerial photography or VIR satellite imagery

Relief Displacement

Vertical structures on radar images, and aerial photographs or VIR satellite images appear to be very different. The most obvious difference is that **relief displacement is in opposite directions**. On aerial photographs and other optical sensor images, relief displacement falls away from the nadir point because the top is imaged further from nadir than the base of a structure. In radar images the top of a structure may be imaged before the base. Thus, the relief displacement falls towards the nadir. Relief displacement will be greater in slant range than ground range due to the fact that the image is more compressed in a slant range presentation. Relief displacement is also most pronounced at near range.

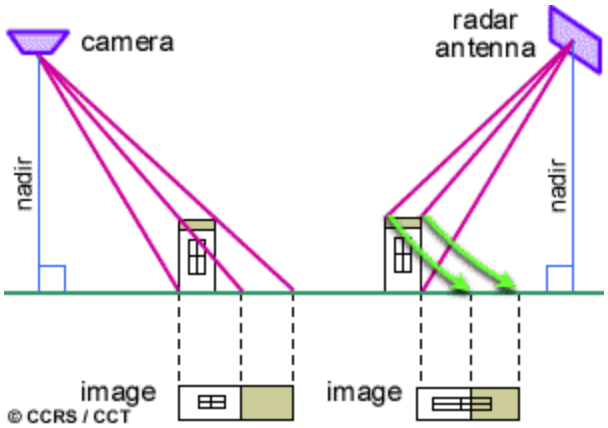

Relief displacements occur in opposite directions for optical andSAR sensors

Range direction distortions on radar images are comparable to those encountered in oblique photographs. But, as can be seen from the previous figure, relief displacements occur in opposite directions for optical and SAR sensors.

The radar perspective represented on an image is portrayed as being orthogonal to the radar direction. Consequently, a viewing angle "η" of less than 90°, usually employed in SAR systems, has approximately the same effect as an equivalent angle of "90°-η"; for oblique optical viewing.

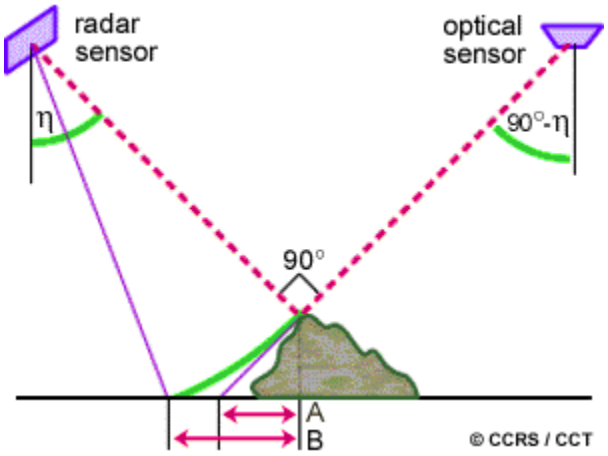

Relief displacement is in opposite directions

A = relief displacement in the direction away from the optical sensor

B = relief displacement toward the radar sensor

η= incidence angle

Keep in mind this relationship. It will help you in understanding the impact of geometry on SAR imagery. For example, it is important when considering stereo configuration and the positioning of SAR stereo image pairs.

The four characteristics resulting from the geometric relationship between the sensor and the terrain that are unique to radar imagery are foreshortening, pseudo-shadowing, layover, and shadowing.

Foreshortening (A'B') is the effect by which the foreslopes of hills and mountains appear to be compressed. The image of foreslopes will therefore appear brighter than other features on the same image. The greatest amount of foreshortening occurs where the slope is perpendicular to the incoming radar beam. The base, slope and top of the mountain will be imaged at the same time and will be superimposed on the image. Foreshortening can be minimized by using a less sharp incidence angle. However, lower incidence angles allow for more shadowing to occur on the image.

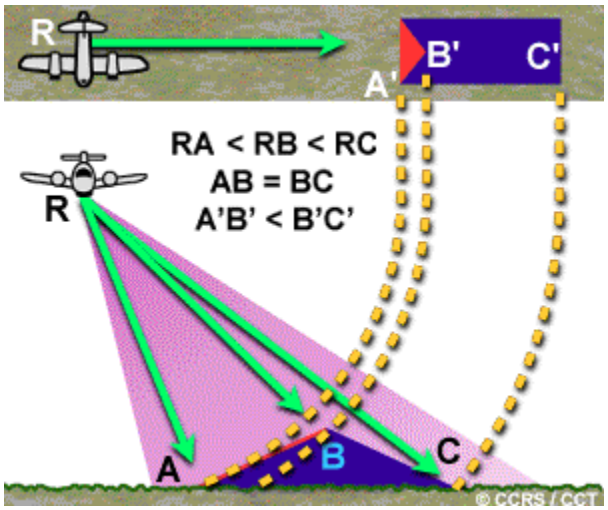

Foreshortening

While the hill slopes AB and BC are equal, the foreslope (AB) is compressed (A'B') much more than the backslope (BC) is compressed (B'C'), due to the radar imaging geometry.

Pseudo-shadowing is an effect by which the backslope of hills and mountains appear to be expanded. It is the result of return signals spread out over a larger distance (A', B') than the actual horizontal distance (A, B). This dispersed return is not always detectable (Leonardo, 1983).

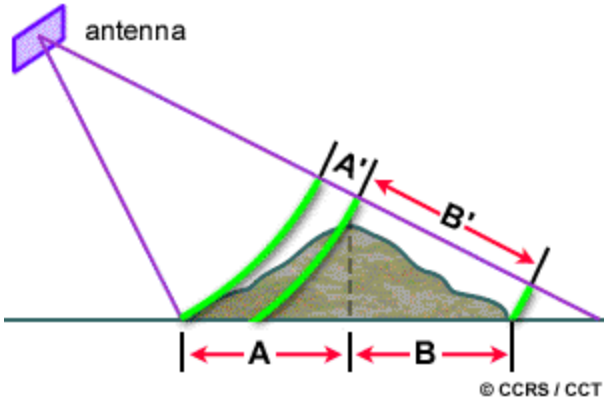

Pseudo-shadowing

A', B' = return signal spread A, B = actual ground distance A'< A B' > B

Layover is the effect where the image of an object appears to lean toward the direction of the radar antenna. It is the result of the tops of objects or slopes being imaged before their bases. Layover effects are most severe on the near range side of images.

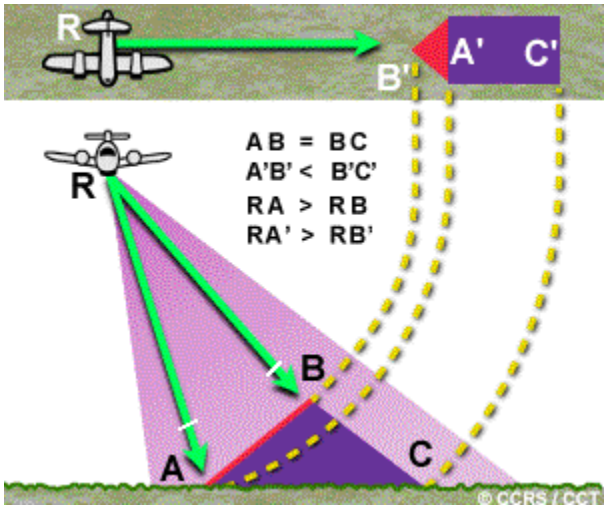

Layover

While the mountain slopes AB and BC are equal, the radar imaging geometry dictates that the radar-facing slope (AB) wil be imaged (B'A') as leaning toward the radar. This is due to the mountain top (B) having been imaged before the base(A) due to RA > RB.

Shadow is very useful to image interpreters interested in terrain relief. As discussed in the first chapter, shadowing is one of the psychological cues used for depth perception. Radar shadows produce a 3-D effect without the use of a stereoscope.

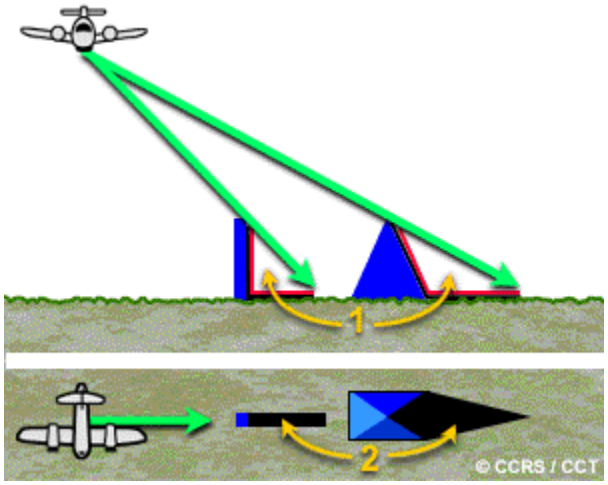

1 = Shadow area not imaged 2 = Radar shadow on image


Example of radar shadow effects under large incidence angle (>45°) illumination.

When terrain slopes are greater than the depression angle, true radar shadows mask down range features. In this case, slopes facing away from the radar antenna will return very weak signals if any. This results in dark or black areas on the image. In areas of high relief, as the depression angle becomes shallower, shadow length increases with range. The shallower the depression angle is on such terrain, the more information will be lost.

Microwave properties

Objects on the Earth's surface react differently with electromagnetic energy. The strength of reflected energy, which is recorded in order to produce a radar image, depends on factors such as:

- the orientation of topographic features,
- surface roughness,
- thickness of surface cover, and
- moisture content / dielectric properties.

It is important to note that microwave reflections from the Earth's surface are not related to their counterparts in the VIR section of the EM spectrum. Surfaces that return a strong signal and are bright in a radar image may return a weak signal in the VIR range of the spectrum and appear dark on a photograph, Landsat or SPOT image.

Surface Roughness

Surface roughness is determined with respect to radar wavelength and incidence angle. A surface will appear to be smooth if its height variations are smaller than one-eigth of the radar wavelength. In general, a rough surface is defined as having a height variation greater than half the radar wavelength. Surfaces will appear to have a greater or lesser degree of roughness, depending on which designated radar bandwidth is used for imaging. In terms of a single wavelength, a surface appears smoother as the incidence angle increases. On radar images, rough surfaces will appear brighter than smoother surfaces composed of the same material.

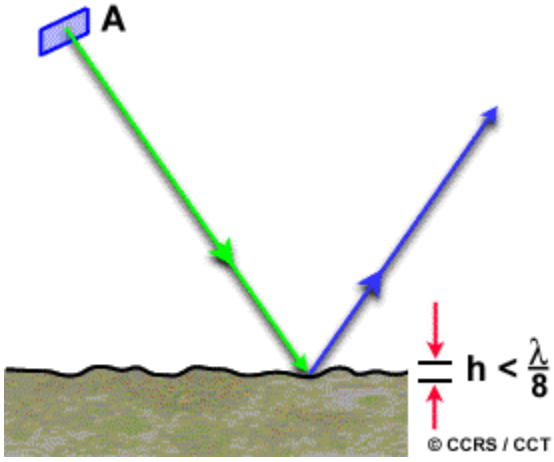

A = antenna; h = height variations of surface; λ = radar wavelength.
Smooth surface; specular reflection; no return.

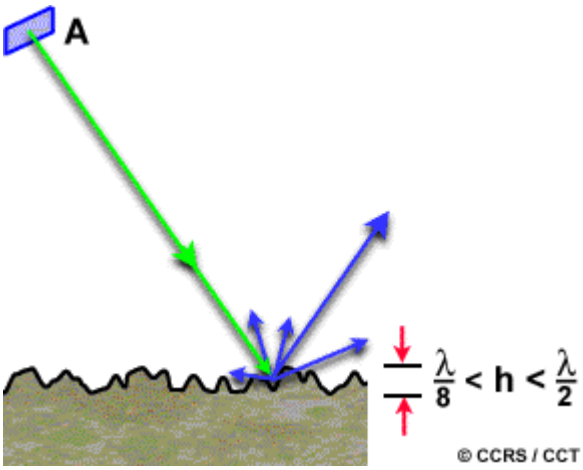

A = antenna; h = height variations of surface; λ = radar wavelength.
Intermediate roughness; mixed scatter; moderate return.

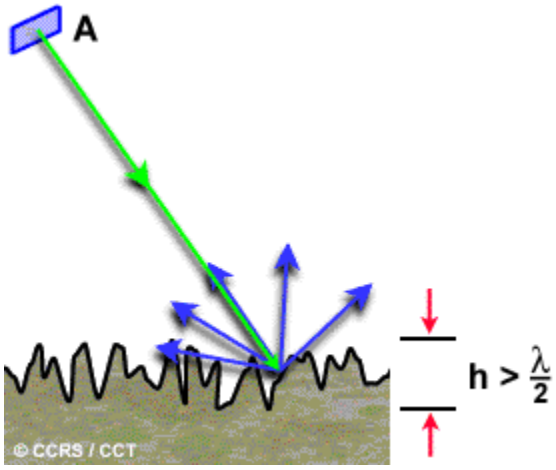

A = antenna; h = height variations of surface; λ = radar wavelength.
Rough surface; diffuse scatter; strong return.

Surface roughness influences the **reflectivity** of microwave energy. Horizontal smooth surfaces that reflect nearly all incidence energy away from the radar are called specular reflectors. These surfaces, such as calm water or paved roads appear dark on radar images.

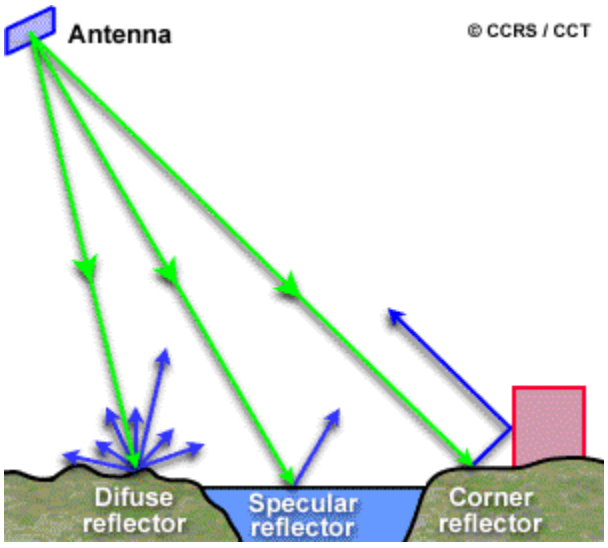

Radar reflection from various surfaces

Rough surfaces scatter incident microwave energy in many directions. This is known as diffuse reflectance. Vegetated surfaces cause diffuse reflectance and result in a brighter tone on radar images.

Moisture Content

The complex dielectric constant describes the ability of materials to absorb, reflect and transmit microwave energy. The dielectric constant increases with the presence of moisture in a material.

Moisture content changes the electrical properties of a material, which in turn affects how the material will **appear on a radar image**. The reflectivity, and therefore image brightness of most natural vegetation and surfaces increases with greater moisture content. Consequently, **soil moisture maps** can be derived from radar backscatter.

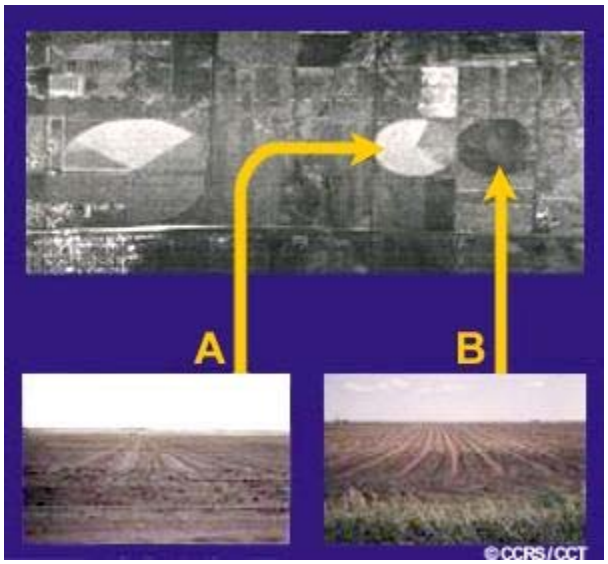

Irrigation / soil moisture influences.

Test site at Outlook, Saskatchewan showing potato fields at pre-emergence stage;
C - VV airborne radar;
A = irrigated field,
B = non-irrigated field.

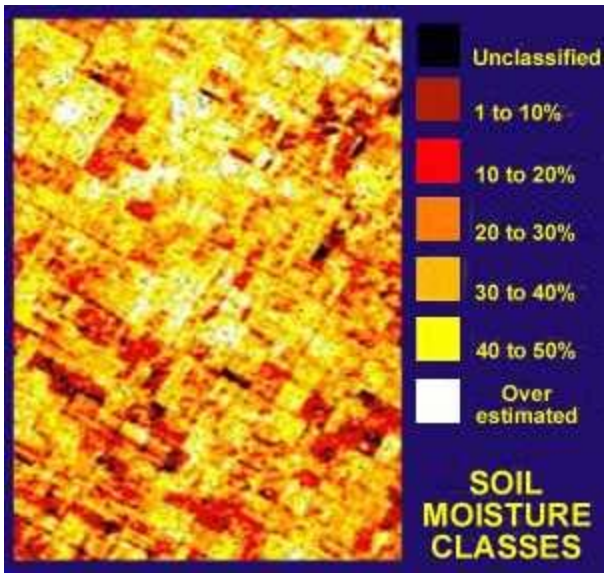

Soil moisture map
near Altona, Manitoba using C band radar data.

Microwaves may penetrate very dry materials such as desert sand. Both surface and subsurface properties affect the resulting scatter. In general, the longer the radar wavelength, the deeper it will penetrate dry material.

Fading and Speckle

Fading and speckle look like grains of salt and pepper randomly distributed on an image. Fading and speckle are noise-like processes inherent in coherent imaging systems. Radar imagery is created with **coherent radar waves** which causes random constructive and destructive interference producing random bright and dark spots in radar imagery. Fading and speckle can be **reduced** by averaging adjacent pixels on radar images, or by designing the antenna to use a multiple look imaging technique.

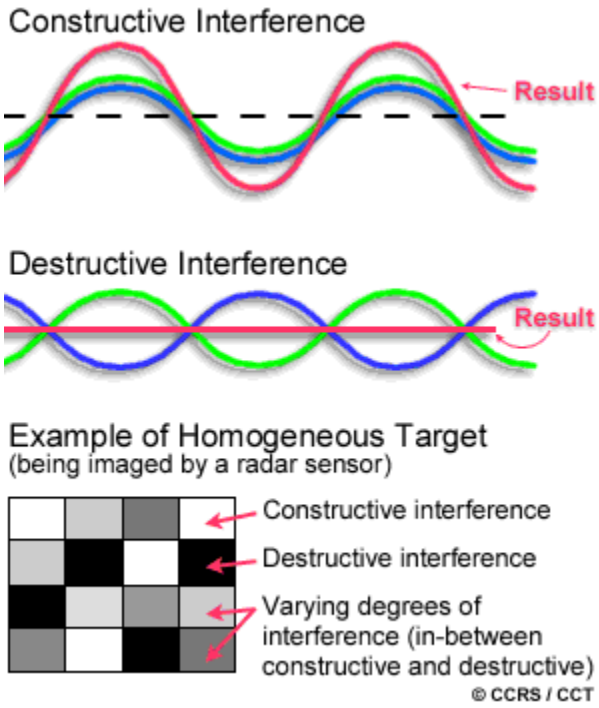

Coherent radar waves

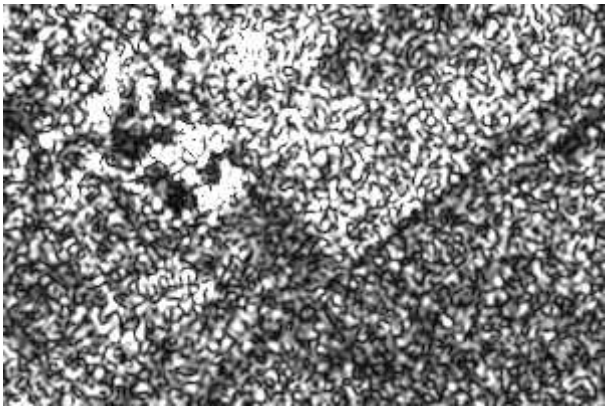

Single look image - high spatial resolution and speckle

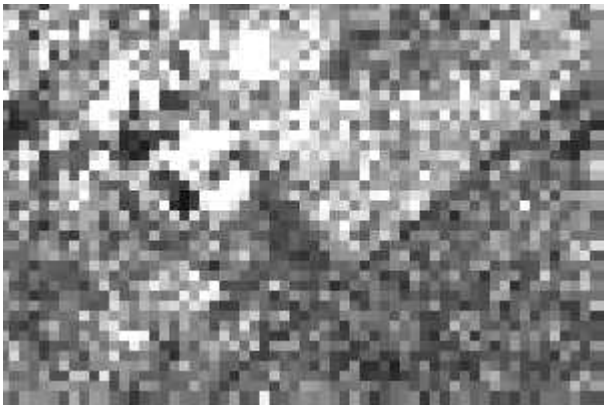

Twenty five look image (five looks in each of x and y directions) - spatial resolution and speckle have been reduced

Fading and speckle can be reduced by averaging adjacent pixels on radar images, or by designing the antenna/processor to use a multiple look imaging technique.

6. RADARSAT Basics

What is RADARSAT?

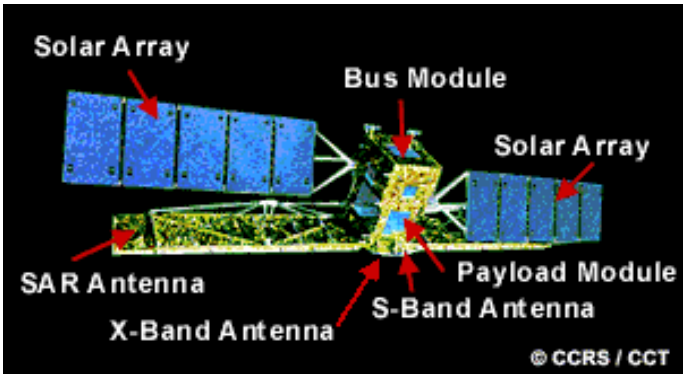

RADARSAT-1 Canada's premier remote sensing satellite

RADARSAT-1 is Canada's first earth-observation satellite. Its launch on Nov. 4, 1995 represented the successful outcome of a program jointly developed by the Canadian Government, provincial governments, and private industry. RADARSAT is a reliable source of data. It produces images that are useful to researchers and operational users working in such fields as:

- Arctic and off-shore surveillance,
- ice, ocean monitoring,
- geology and geologic hazard monitoring
- agriculture,

- cartography,
- hydrology,
- forestry, and
- mapping.

6.1 The RADARSAT System

How does the RADARSAT system work?

RADARSAT is an active remote sensing system employing a Synthetic Aperture Radar (SAR) sensor, which transmits and receives microwave energy to and from the Earth's surface. The return signals are recorded and processed to produce radar imagery. RADARSAT operates on a single **microwave** frequency of 5.3 GHz (a 5.6cm wavelength), known as the C-band with a horizontal polarization for the emitted and received signals. Microwave energy can be transmitted and received through darkness, cloud cover, rain and snow, dust or haze, allowing RADARSAT to collect data under any atmospheric conditions.

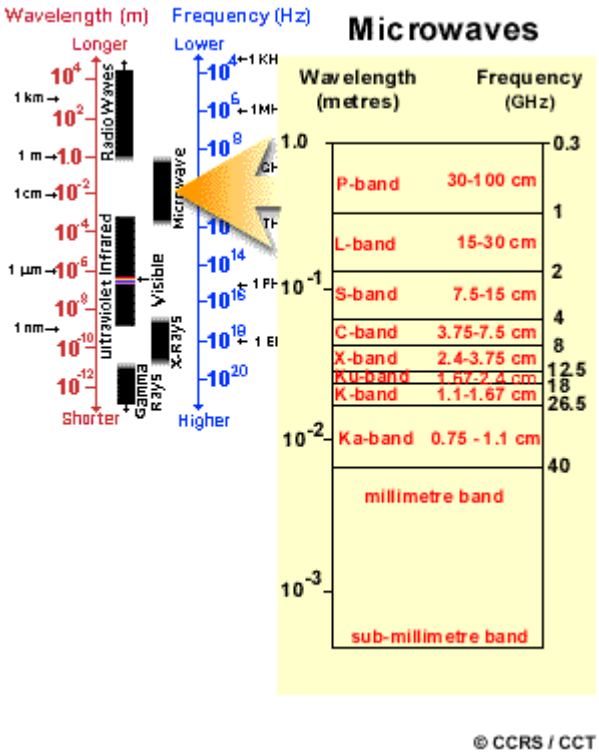

The Microwave portion of the electromagnetic spectrum

RADARSAT is a sun synchronous satellite that travels at an altitude of approximately 800 km above the Earth's surface. It crosses the equator at dawn and again at dusk. This allows its solar array to be in almost continuous sunlight and enables it to function mainly on solar rather than battery power. RADARSAT has an orbital period of 101 minutes and circles our planet about 14 times a day. Its orbital path cycle repeats itself every 24 days, which means the same image (same beam mode, same beam position, same geographical

location) can be collected every 24 days. However, data over the same area can be acquired over several days as beam positions change.

More technical details on RADARSAT are available on the CCRS Website.

6.2 Data Acquisition

How are data acquired?

Users place an imagery order with one of the order desks by specifying parameters such as look direction, beam mode and beam position. This allows users to choose the area of coverage, the image resolution and the image geometry best suited to their needs. Choices can be made from two look directions, seven operational beam modes, and a range of beam positions. Orders are forwarded to Mission Management Office at the Canadian Space Agency (CSA). Here the various user orders are reconciled and an acquisition schedule is prepared. The CSA Mission Control Centre creates the imaging instructions for the SAR and transmits them to the satellite via their Tracking, Telemetry and Control Antenna. The data are received at either the Prince Albert or **Gatineau** receiving stations.

Look Directions

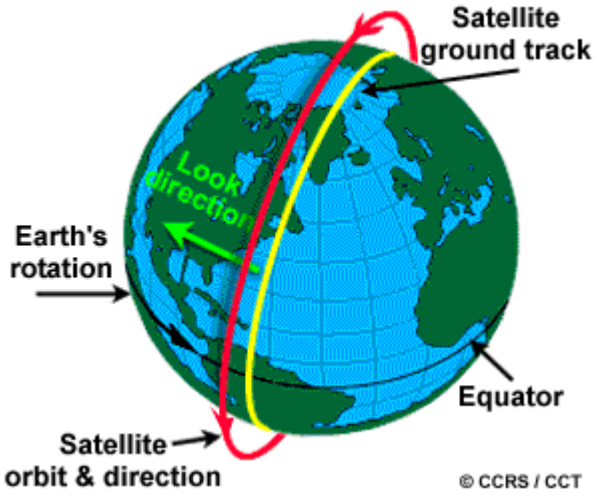

RADARSAT-1 orbit and look direction

RADARSAT is a **right looking satellite**. However, as it orbits the planet it has two look directions relative to the Earth's surface. As it descends from the North Pole it faces west. As it ascends from the South Pole it faces east. Thus a geographical area can be imaged from opposite sides.

Operational Beam Modes

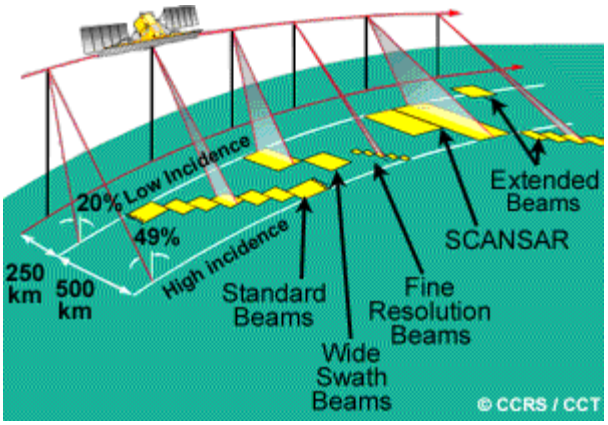

RADARSAT-1 beam modes

RADARSAT can collect data from a **variety of beam modes**. Each beam mode is defined by the area of ground coverage and by the level of detail or resolution it can provide. The beam modes range from Fine mode which covers an area of 50 km2 with a nominal resolution of 10 metres to ScanSAR wide which covers a 500 km2 area with a nominal resolution of 100 metres. Standard mode covers a 100 km2 swath with a nominal resolution of 30 metres.

Beam Positions

Within each RADARSAT beam mode, a number of beam positions are available. Each beam position is defined by a near and far edge incidence angle. This is the angle between the radar beam and the flat Earth's surface. Beam positions range from shallow to steep. The Fine mode has five beam positions with incidence angle pairs ranging from 37 to 40 degrees to 45 to 48 degrees, while Standard mode has seven ranging from 20 to 27 degrees to 45 to 49 degrees.

RADARSAT's ability to collect data from a variety of beam modes, positions and two look directions is a real advantage to image interpreters. Different combinations will enhance specific features of interest to users. This is especially true if the user wishes to generate a stereo pair.

6.3 RADARSAT and Stereoscopy

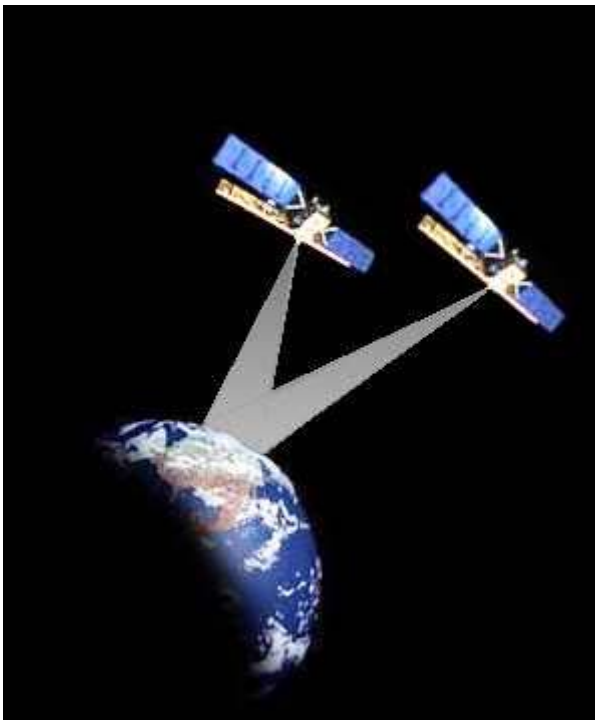

RADARSAT-1 for stereo imaging

The stereo parallax necessary for a stereo image pair or an anaglyph is created when an object is viewed from **two different positions**. As with aerial photos, RADARSAT and other satellite image pairs are sequenced from left to right depending on the position of the platform at the time the image was taken. The sequence of a RADARSAT image pair depends on two factors:

- beam position of the sensor, and
- whether the satellite was on an ascending or descending orbital pass.

As noted previously, RADARSAT has the ability to collect data from a range of beam positions. The beam position sets the viewing angles. These are steepest at the first, and shallowest at the last position. On an ascending pass the look direction of the sensor is to the east. The beam positions fan out sequentially towards the east. On a descending pass the sensor faces west and the beam positions fan out towards the west.

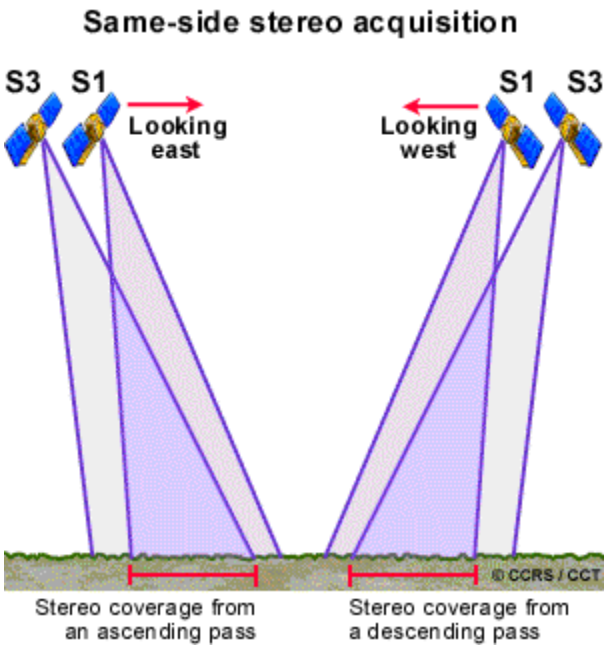

Two examples of same-side stereo acquisition
using S1 and S3 beam modes of RADARSAT-1

For example, in order to image the same geographical area with an S1 and S3 beam mode and position, both on a descending pass, the S3 satellite orbit will be east or to the right of the S1 satellite orbit. This is due to the fact that S3 has a shallower viewing angle than S1. Thus, the S1 image will take the left hand position of an **S1/S3 image pair** collected on a descending pass. If both images are collected on an ascending pass, the order of the image pair is reversed.

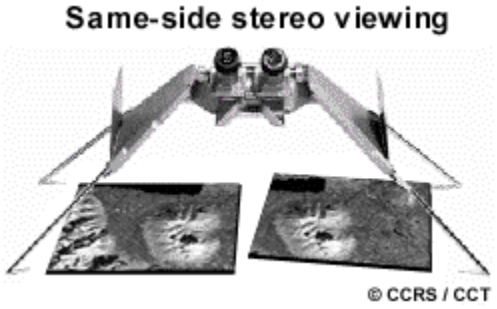

Example of same-side stereo viewing
using S1 and S3 beam modes of RADARSAT-1

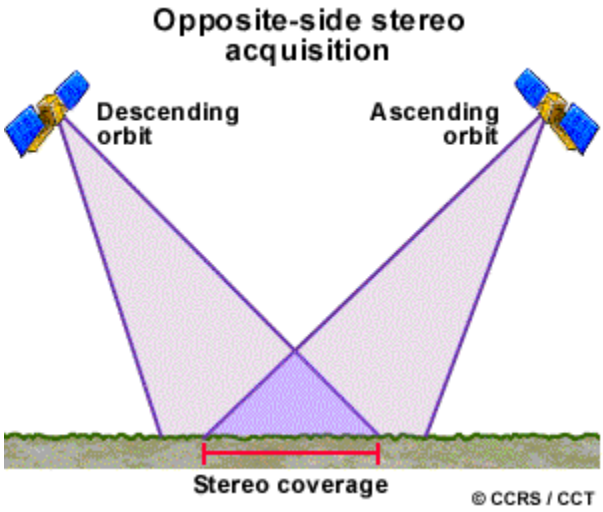

Opposite-side stereo acquisition for RADARSAT-1

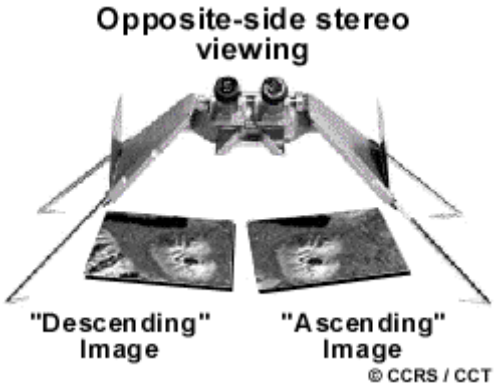

Opposite-side stereo viewing

In the case of an **opposite-side stereo** configuration the descending image is **viewed** on the left hand side while the ascending image is viewed on the right hand side. Such an example is given with descending/ascending ERS-1 images in chapter 7. This sequence may seem reversed to viewers accustomed to viewing optical imagery. However, if we recall that on SAR images, relief displacement is towards the sensor, while on optical images relief displacement is away from the optical sensor, the order makes sense. Remember that a SAR viewing angle, η has approximately **the same effect** as an equivalent oblique optical viewing angle of 90°- η.

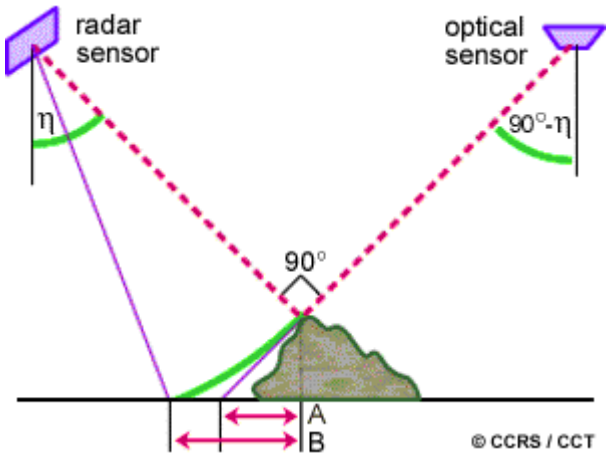

Angle of view

7. Stereo Interpretation

The purpose of this chapter is to illustrate how a stereoscopic apparatus is used to view and interpret RADARSAT data in stereo. Data sets, from RADARSAT and other sources, will be used as examples to show:

- three different methods of representing depth information,
- possibilities of creating stereo image pairs from different data sources,
- different look directions, beam modes and beam positions of RADARSAT data available to the user,
- effects of ground cover, terrain, and geographical location on RADARSAT image pairs, and
- different image processing techniques that enhance the viewability of RADARSAT stereo pairs.

Stereoscopic viewing

The objective here is to build practical experience using theory provided in previous chapters of this manual with examples of RADARSAT and other data sets. The user will gain a practical understanding of the geometric and radiometric differences between different data sets. This will include the way in which parameters related to satellites, sensors, Earth location and image processing techniques are affected by those differences. Furthermore, information presented in this chapter will enable users to generate the best stereo pair according to the data set, study site and thematic application that they are currently working with.

Section 7.1 is a comparison of RADARSAT stereo image pairs with other platform and sensor image pairs. Data acquired by aerial photography, airborne SAR, SPOT and ERS-1 satellites will be compared with RADARSAT data in terms of geometry. In the case of sensors, image pairs obtained with a camera, VIR scanners and other SAR systems will be compared with RADARSAT images in terms of radiometry. Part 2 also contains examples of mixed sensor pairs such as SPOT/Landsat and ERS-1/JERS-1. These are included to demonstrate the possibilities of using data from different sources to generate depth perception. The geometry and radiometry of each mixed sensor pair will be compared.

In Section 7.2, stereo viewing of RADARSAT images will be addressed. Sensor parameters such as beam modes, beam positions, and look directions and ground considerations such as terrain type and geographical location will be considered.

Some effects of sensor parameters and ground considerations include:

- the amount of area that can be seen in stereo,
- the amount of detail that can be seen in stereo, and
- whether layover, foreshortening or shadowing present a barrier to effective stereo viewing.

To illustrate these factors RADARSAT stereo pairs, which are easily viewable in stereo will be compared with those, which are not.

In Section 7.3, problems that affect stereo viewability, but can be corrected by simple image processing techniques, will be discussed. Scale differences between image pairs, due to differing sizes of the data sets or to a slant range representation, can be corrected. Rotations can be done in order to allow the viewer to see an image pair in stereo with greater ease. An antenna pattern correction can be applied to an image where the antenna pattern interferes with the ability to see the image pair in stereo. Filtering techniques can be used to reduce speckle. Examples of image pairs, where these image processing tools have been used, will be discussed.

When viewing stereo image pairs it should be remembered that it will be easier to perceive depth in some pairs than in others. Viewing a stereo pair of aerial photos or SPOT satellite images will seem easy and "natural" because these are optical systems. Our eyes and consequently our brain perceive objects as optical systems do. Initially, SAR image pairs may be more difficult to view in stereo. This is due to humans not "seeing" as a SAR system does. We are not sensitive to microwave energy. Nor do we "illuminate" the objects we are looking at as bats and dolphins do using sound waves. Psychological cues, such as shade and shadow, which we rely on, are different on optical and SAR images.

It may take our brains a little time to integrate new information. Practice makes "perfect". With experience, SAR image pairs can be viewed in stereo as easily as aerial photographs. Additional experience enables us to view even mixed sensor pairs in stereo. People trained and experienced in stereo viewing may have a greater facility to perceive depth in challenging stereo pairs. Do not give up.

7.1 Image Type Comparisions

A Comparison of RADARSAT data and data obtained by other platforms and sensors.

7.1.1 Airborne versus Spaceborne Platforms

This section will compare aerial photographs, airborne SAR images, SPOT, ERS-1, and RADARSAT image pairs. Aerial photography has traditionally been used for stereo viewing. Various airborne SAR systems such as the CCRS CV-580 and Intermap's Star 1 & 2 systems have collected images for use in stereo. ERS-1 imagery can be viewed in stereo from an opposite side configuration. SPOT and RADARSAT satellite systems are easily adapted for stereo usage. The stereo pairs will be compared in terms of geometry, as it is the first distinguishing element between different imaging platforms.

Stereo pair 1 - RADARSAT - Bathurst Island, Nunavut, Canada

This image pair is very easy to view in stereo. Vertical exaggeration is pronounced and accentuates subtle differences in relief. In the stereomodel, ridges appear to be deeper and folds appear higher than they are in reality. The elevation difference of the terrain pictured in this image is 150 to 200 metres. The topography is the result of a very long erosion process, which has worn down mountains but has left valleys intact.

Stereo pair 2 - SPOT - Okanagan Valley, British Columbia, Canada

The stereomodel resulting from this image pair is similar to one provided by aerial photographs. This is due to the fact that SPOT is an optical system. Change in elevation in this area, from the surface of Lake Okanagan to the top of Isintok Mountain (bottom right of both images) is approximately 2000 m. Slopes are steep. Slopes leading down to the valley bottom through which the highway and railway run are in the range of 50 per cent. However, there is some vertical exaggeration in this stereo pair. Slopes appear steeper than they are in reality. For example, Mt. Acland appears to rise almost vertically. Vertical exaggeration is due to the large intersection angle formed by this stereo pair.

Stereo pair 3 - ERS-1 - Sudbury, Ontario, Canada

This image pair is difficult to view in stereo. The terrain is characterized as being one of rolling topography. The elevation ranges from 300 to 500 m and slopes are generally no greater than 10°. Throughout the image area foreshortening and shadow effects are reduced, due to the shallow slopes. In some specific areas these double bounce reflection effects occur along road or forest borders and interfere with stereo viewing locally. The opposite side configuration causes these effects to be on opposite sides on the images and adds to the difficulty of effective stereo viewing. Vertical exaggeration is not evident in this image pair.

Stereo pair 4 - Airborne SAR - Cerro Planatar, Costa Rica

These images were acquired by the CCRS CV-580 in nadir mode. A full stereomodel can be viewed with this image pair, but can be confusing at first glance. The viewer is advised to focus on the flatter areas first and then to view the mountains. Otherwise, the stereo overlap will appear to slope steeply towards the near edges of the stereo image pair. There is some vertical exaggeration. The volcano in the top half of the images appears to be greater in height than its actual 2000 m.

Stereo pair 5 - Aerial photography - Bathurst Island, Nunavut, Canada

Vertical exaggeration is less pronounced than in the RADARSAT image pair. The aerial photos show a more realistic image of Bathurst Island's topography. However, they are at such a large scale that it would take many image pairs to cover the area of one RADARSAT stereo pair.

7.1.2 Optical and VIR sensors versus radar sensors

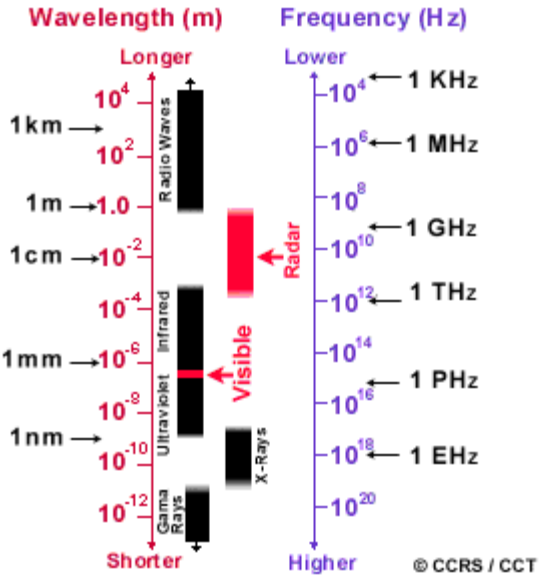

The stereo pairs will now be compared in terms of the qualitative information they give. This is expressed by the image radiometry, which is a measure of the power of the return signals. In radar systems, the power of the return signals is dependent on the type of surface the transmitted signal encounters. As outlined in previous sections of this tutorial, ground moisture, the presence of vegetation, and terrain topography are all factors affecting the return signal strength. On SAR images, the range of greys represents the strength of return signals. The brightest greys (white) represent the strongest return signals, while the darkest greys (black) represent the weakest, or no return signal. In aerial photographs and SPOT and Landsat VIR images, the power of reflected visible light is represented by a range of greys for each channel.

Stereo pair 1 - RADARSAT - Bathurst Island, Nunavut, Canada

On the images there is a very strong contrast between land, water, and different types of rock units. Bodies of water and landforms are clearly delineated. Different geological formations can be easily identified. Sensitivity to roughness is indicated by rougher terrain returning brighter signals than smoother terrain. Incidence angle effects such as foreshortening, layover and shadowing are not evident due to the nature of the land surface. Seasonal vegetation differences cannot be identified since these images were taken within days of each other.

Stereo pair 2 - SPOT - Okanagan Valley, British Columbia, Canada

These two images are very similar radiometrically. The only pronounced contrast on the images is between cleared and forested areas. Cleared areas include the road network, cut lines, hydro lines and areas with a slope too steep to support tree growth. Vegetation seasonality cannot be easily distinguished due to the black and white nature of the images.

Stereo pair 3 - ERS-1 - Sudbury, Ontario, Canada

There is a great deal of variation in radiometry between the two images. This difference is largely due to the images being collected from ascending and descending passes which means the images were taken during the day and at night. Since there is generally less wind at night, water/land boundaries may appear different than an image that was taken during the day. Both images contain speckle. Some double bounce reflection effects are visible causing bright returns in some areas. These bright areas interfere locally with stereo-viewing. Soil moisture can be distinguished. Lower lying wetlands are evident. Vegetation seasonality cannot be identified since the images were taken within six days of each other.

Stereo pair 4 - Airborne SAR - Cerro Planatar, Costa Rica

The contrast between different land features ranges from medium to strong on these images. Sensitivity to roughness is shown by different return signals from different ground cover types. Forested areas are rougher than agricultural fields. Both are easily distinguished. Forested areas are brighter than agricultural areas. There is some brightness due to foreshortening. Speckle is minimal.

Stereo pair 5 - Aerial photography - Bathurst Island, Nunavut, Canada

There is a medium contrast between water, land and rock units. Rougher terrain is visible in an optical sense since the scale of the image pair is large. Graininess is not evident. Soil moisture and vegetation seasonality cannot be easily distinguished due to the nature of black and white photography.

7.1.3 Mixed Sensor Pairs

Several mixed data stereo pairs will be presented in this section. These image pairs have been included to demonstrate the possibility of viewing an area in stereo, given two different data sets. The viewing geometry and radiometry of each mixed data pair will be shown.

Although a mixed sensor pair may be difficult to view in stereo at first glance, with practice it becomes easier. The optical imagery of SPOT and Landsat can be viewed in stereo with little difficulty. SAR imagery, in combination with optical imagery, presents a greater challenge. However, with practice, the stereo effect produced by two different views of the same geographical area, is visible even with these very different types of imagery.

Stereo pair 6 - ERS-1/JERS-1 - Indonesia

This image pair is very easy to view in stereo, however, the resulting stereomodel is distorted. For example, the volcano appears to lean toward the sensors. This is very different from the traditional bird's eye optical view. Contrast on the images is strong, and is due largely to foreshortening and shadow. These effects dominate this image pair. There is strong variation between the images. Layover is greater on the ERS-1 image because of the steeper viewing angle. Shadow provides important cues in allowing the viewer to identify lava flows and river/stream networks. Both images contain speckle, which makes the viewing of detail a little more difficult.

Stereo pairs 7a & 7b - SPOT/Landsat - Okanagan Valley, British Columbia, Canada

While all three images are close in radiometry, greater contrast exists on the Landsat-TM image. In general, the images do not contain a great amount of contrast, except between forested and cleared areas. The road networks are bright against the grey surroundings. The sensor is not sensitive to roughness. There is minimal graininess. The Landsat image contains some cloud cover, which interferes with stereo-viewing. Overall, it is very easy to view these images in stereo. The most obvious point of comparison between these two image pairs is that the first (PLA26/TM) has a much more pronounced vertical exaggeration than the second (TM/PLA10). This is due to the larger intersection angle of the PLA26/TM image pair.

Stereo pair 8 - ERS-1/SPOT - Okanagan Valley, British Columbia, Canada

This image pair is very difficult to view over the full area due to many distortions between the images. Thus, the viewer is able to see only small areas at a time. Each image contains some contrast, but between different features. On the SPOT image, roads, cleared areas and rock faces contrast with trees and other vegetation cover. On the ERS-1 image, contrast occurs as a result of the relationship of topography and incidence angle effects. For foreslopes greater than 23º foreshortening and layover occur. Where backslopes are greater than 67º shadowing occurs. On this image, foreshortening and layover dominate. Where cleared areas are visible, they are dark in comparison to the surrounding tree cover. Forested areas return a stronger signal than the cleared areas and therefore, appear brighter on the image. There is a high amount of speckle on the ERS-1 image. Different geometry and radiometry of these two images interferes with effective stereo viewing.

A mixed sensor image pair such as this presents the greatest challenge to stereo viewing. With training and practice, the brain can learn to perceive depth in an image pair collected from very different sources. The more experienced a person is with stereo, the greater their ability is to view image pairs acquired from different sources.

7.2 RADARSAT Stereo Images

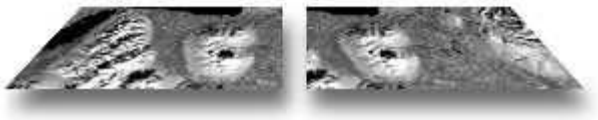

In the following section we will compare RADARSAT images of different terrain types, geographical latitudes and stereo configurations. Each of these factors affects the amount and quality of information we can extract from a **RADARSAT image pair**.

7.2.1 Terrain Type

Terrain Type - Mountainous

Stereo pair 9 - RADARSAT - Okanagan Valley, British Columbia, Canada
This image pair covers approximately 2/3 of a full Fine mode scene of the Okanagan Valley, B.C. area. This area was chosen to correspond to the area shown in the SPOT, Landsat and ERS-1 images of Stereo pairs 2, 7 and 8. Geometry inherent in a radar remote sensing system such as RADARSAT is illustrated very well in this example. Effects of foreshortening, layover and shadowing are clearly visible. Mt. Acland (just right of centre on both images) is compressed on the west face and appears to lean towards the sensor. Layover is visible along the ridge running parallel to Lake Okanagan. Due to a much smaller intersection angle vertical exaggeration in this stereo pair is much less pronounced than in the SPOT imagery (Stereo pair 2).

Much of the contrast on these images is also due to geometry. Sides of mountains facing the sensor appear bright while those facing away from the sensor are in shadow. There is a strong contrast between land and water. Cleared areas, such as the hydro line, roads and fields appear darker than surrounding forest coverage, which is brighter. Seasonal vegetation differences cannot be distinguished as the data was acquired 2.5 weeks apart. Speckle is this scale.

Terrain Type - Rolling

Stereo pair 10 - RADARSAT - Ottawa, Ontario, Canada

The area covered by the images over Ottawa is characterized by the Gatineau Hills to the north, the Ottawa River Valley and flat lands to the south. Change in elevation between the river valley and the Gatineau Hills is approximately 300 m. The relief of the Gatineaus Hills, is clearly visible as is the rise from the Ottawa River. Vertical exaggeration is pronounced. The Gatineau Hills appear to be almost mountainous. The two images do not contain a large amount of contrast, however there are variations in contrast between them. The S1 image shows a stronger contrast between land and water bodies than the S3 image. However, S3 shows stronger contrast between ground cover types than S1. These radiometric differences can be explained by the difference in acquisition dates - S1 on Dec. 12, 1995 and S3 on Feb. 13, 1996. Therefore land/water boundaries are less delineated on the S3 image due to ice. Fields are brighter on the S1 than the S3 image because the snow was very dry in Dec. 1995 and very wet in Feb. 1996. These differences in radiometry interfere slightly with stereo-viewing.

The S1 image shows more foreshortening and layover effects than the S3 image. This is due to the steeper S1 viewing angle. Speckle is minimal on both images.

Terrain Type - Flat

Stereo pair 11 - RADARSAT - Tapagos Forest, Brazil

This area is characterized by a change in elevation of less than 50 m. Change in relief between the coastal area and the inland plateau can easily be seen. Differences in height between the top of the tree canopy and fields cleared for agricultural crops can also be seen.

The two images are very similar radiometrically. The images were collected at the same time of the year. The incidence angle has little impact on either image as the land surface is almost completely flat. There is a weak contrast on the images. Land and water bodies are sharply differentiated. Some contrast is due to shadow. The ridge of the plateau and small stream beds are delineated by shadow.

There is evidence of sensitivity to roughness in the difference between agricultural crops and forest. Forested areas are a little brighter than agricultural fields. The images contain some speckle, which interferes with sharpness on the images. Fields or clear cut areas would be more clearly delineated with less speckle. Both images were collected at the same time of the year therefore seasonal changes in vegetation cannot be identified.

Changing the order of this stereo pair should lead to a pseudoscopic stereomodel. However, with this stereo pair some people will still see a normal stereomodel. This is due to psychological cues (shadow on both images), which are stronger than physiological cues (binocular disparity) on images of flat terrain.

7.2.2 Geographical Latitude

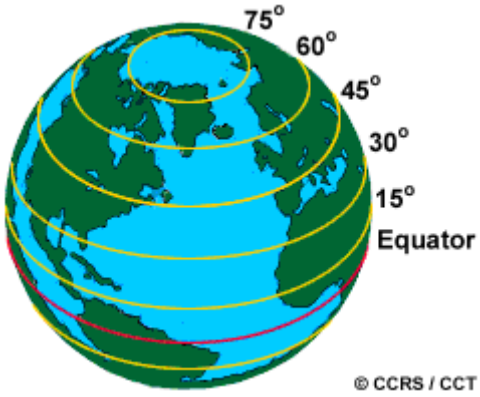

Geographical Latitude - Northern

Stereo pair 1 - RADARSAT - Bathurst Island, Nunavut, Canada

Since Bathurst Island is at approximately 75º North, the convergence angle between the orbital tracks is quite large. As a result the right hand image must be manually rotated with respect to the left hand image. In this case the rotation is approximately 13º.

Geographical Latitude - Mid-Northern

Stereo pair 10 - RADARSAT - Ottawa, Ontario, Canada

The area covered by the images over Ottawa is approximately 45º North. In order to view these images with the stereoscope, a very small manual rotation of the right hand side image is done with respect to the left hand image.

Geographical Latitude - Equator

Stereo pair 11 - RADARSAT - Tapagos Forest, Brazil

These images are of an area of Brazil at 3º South of the Equator. No rotation is necessary.

7.2.3 Stereo Configuration

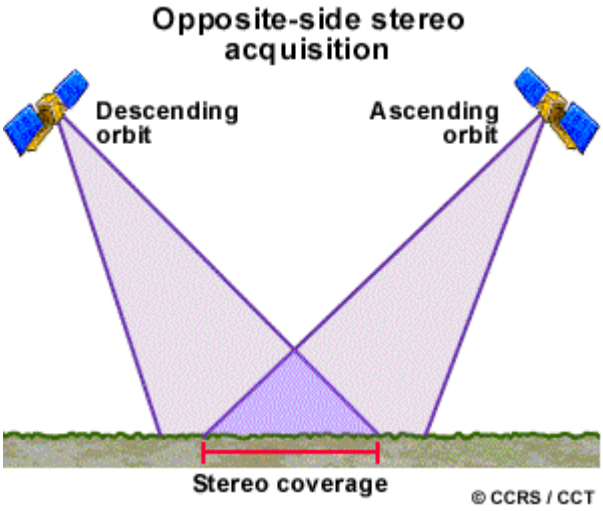

Stereo configuration: Opposite side

The two image pairs considered were F2/F1 (Stereo pair 12) and F4/F5 (Stereo pair 13) collected on descending/ascending passes respectively. At this latitude, (approximately 45º North), the convergence angle between ascending and descending orbital passes is between 20º and 25º. To compensate for this, the images must be rotated with respect to each other in order to obtain the stereo-model. These image pairs are very sensitive to mis-orientation. Once the images have been oriented correctly, the viewer will notice that compared to a same side image pair, a smaller image area is viewable in stereo.

Stereo pair 12 - RADARSAT - Sherbrooke, Québec, Canada

Vertical exaggeration is pronounced in both image pairs (Stereo pair 12 and 13) due to large intersection angles. Thus, on these images, the topography around Sherbrooke appears to have much greater changes in elevation than the actual 250 m. The vertical exaggeration is more pronounced in the F2/F1 image pair since F1 and F2 viewing angles are steeper than F4 and F5 viewing angles. Stereo parallax is greater for steeper viewing angles. Elevation distortions increase with steepness of viewing angle.

The radiometry of all four images is very similar. There is a strong contrast on each image allowing lakes, rivers, roads, and even a ski hill to be identified. Forests and agricultural areas are easily distinguished due to the sensor's sensitivity to roughness. Seasonal changes in vegetation can be identified when comparing the F1, F2, F4 images with the F5 image. The F5 image was acquired in June1996, while the former three were all acquired in October, 1996. Soil moisture is difficult to identify without some knowledge of the land use/cover of the area.

The F2/F1 images display more foreshortening effects than the F4/F5 images. This is expected because the viewing angles of the former are steeper than the latter.

Stereo pair 13 - RADARSAT - Sherbrooke, Québec, Canada

The first attempt at viewing these two image pairs (Stereo pair 12 and 13) may be confusing. The opposite side stereo configuration causes foreshortening and shadow effects to appear on opposite sides of land features in areas where slopes are greater than the viewing angles. Depending on the individual viewer, foreshortening cues may overpower shadow cues and brighter aspects dominate darker ones, or vice versa. This means that, at first, it will not be easy to see the depth of valleys or the heights of mountains in those local areas. However, with practice we can learn to be comfortable with these opposing effects. Depth information will be taken from the dominant cue. We can learn to see large differences in relief very well with an opposite side stereo configuration. Where the topography is rolling, stereo viewability is much easier. The viewer is encouraged to practice with the F2/F1, F4/F5 image pairs and to try the F2/F5 and F4/F1 combinations on their own.

Stereo configuration: Same side

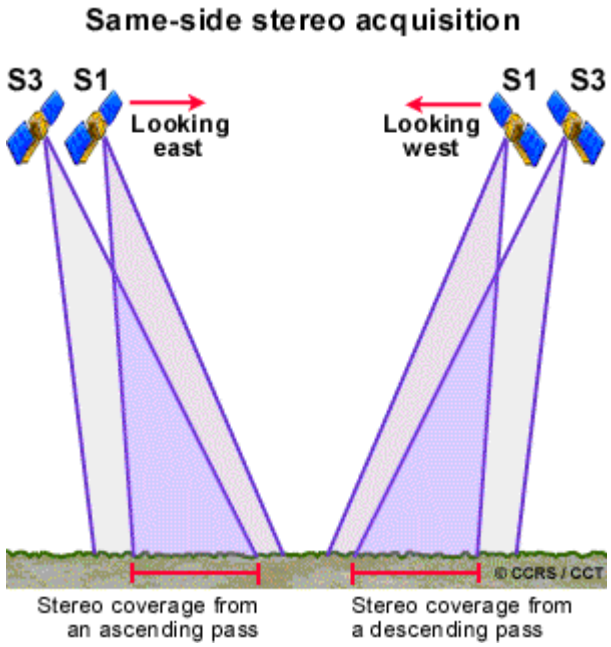

Stereopairs 12A & 13A - RADARSAT - Sherbrooke, Québec, Canada

The F1, F2, F4 and F5 used in the opposite side configuration combinations (Stereo pairs 12 and 13) can also be used to generate two same side stereo image pairs: 12A and 13A. F5/F1 (Stereo pair 12A) is from an ascending pass and F2/F4 (Stereo pair 13A) from a descending pass. The radiometric aspects of these image pairs are discussed on the Stereo pair 12 and on Stereo pair 13 pages.

These image pairs are easier to view in stereo than the opposite side combinations. A larger image area is visible (at any one time) in stereo since the images do not have to be rotated with respect to each other. The most obvious difference between these two same

side image pairs and the opposite side combinations is that a same side stereo configuration does not produce the same amount of vertical exaggeration. Both of these image pairs display a much more realistic visualization of topography in the Sherbrooke area.

Due to larger intersection angles a stronger perception of relief is given in the F5/F1 image pair than in the F2/F4 pair.

Stereo configuration: Same side - Steep viewing angle

Stereo pair 14 - RADARSAT - Sherbrooke, Québec, Canada

This image pair is very easy to view in stereo. However, due to the relative steepness of the viewing angle, foreshortening and layover effects are noticeable. The ridge in the top half of the stereomodel appears to lean towards the sensor. Vertical exaggeration is pronounced. Standard mode viewing angles are steeper than Fine mode viewing angles so that vertical exaggeration in this pair is more evident than in the Fine mode pairs discussed in the previous pages.

Stereo configuration: Same side - Shallow viewing angle

Stereo pair 15 - RADARSAT - Sherbrooke, Québec, Canada

This image pair is also easy to view in stereo. Since S7, the shallowest of the standard mode viewing angles, is used in this image pair, foreshortening and layover effects are less pronounced and shadow effects are stronger than in Stereo pair 14.

Stereo configuration: Same side - Small intersection angle

Stereo pair 10A - RADARSAT - Ottawa, Ontario, Canada

In addition to the S1 and S3 images which make up stereo pair 10, S2 and S7 images were also made available. These four images can be combined in order to generate stereo pairs 10A and 10B once they have been re-scaled to a common size. (Resizing is discussed in Part 4 of this chapter.) Stereo pair 10A was created from the S1 and S2 images. The radiometry of the Ottawa image pairs has been discussed previously. The most obvious feature of this image pair is that there is less vertical exaggeration than on the S1/S3 pair discussed previously and the S1/S7 stereo pair to be discussed next.

Stereo configuration: Same side - Large intersection angle

Stereo pair 10B - RADARSAT - Ottawa, Ontario

Stereo pair 10B was created from the S1 and S7 images. As with the S1/S3 and S1/S2 Ottawa image pairs, the Gatineau Hills and the Ottawa River valley are easy to see in relief. Relief on both sides of the river is more pronounced than in the S1/S3 and S1/S2

image pairs. Of all the same-side stereo Ottawa image pairs discussed thus far, this pair shows the greatest stereo effect. Vertical exaggeration is more pronounced in this image pair due to the greater intersection angle.

7.2.4 Beam Mode

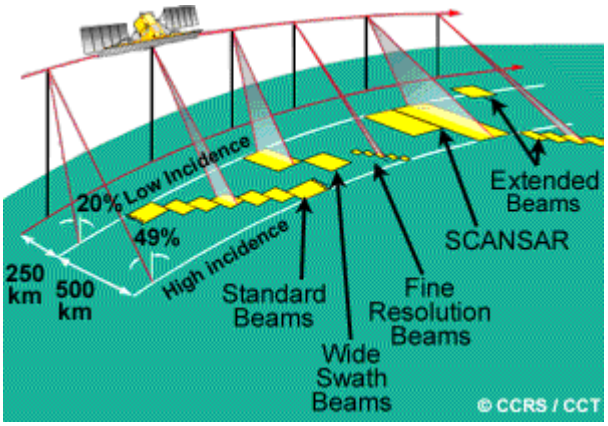

Standard versus Fine mode

The examples in this section include two data sets acquired over the Sherbrooke, Que. area. The first, used in Stereo pairs 12, 13, 12A and 13A was acquired in Fine mode. The second, used in Stereo pairs 14 and 15 is in Standard mode. Obviously, the Fine mode data shows us more detail than Standard mode. This is advantageous if users are required to identify fine details for their particular application. Fine mode data contain more speckle than Standard mode data because one-look rather than four-looks signal processing is applied.

Fine Mode Stereo Pair

Stereo pair 12A - RADARSAT - Sherbrooke, Québec, Canada

This stereo pair (F5/F1) is generated from ascending path, fine mode images. It displays much more cartographic detail, due to SAR resolution cells of about 8m. For example, most of the roads are clearly visible and can be easily extracted with small omission errors (less than 10%) and with a 10m positioning error depending on the type and size of the roads (Toutin, 1998 b). Since the SGF RADARSAT format images were resampled with 6.25m pixel spacing, they are under-sampled when compared to the resolution cell. The SGX RADARSAT format images, which are oversampled (3.125m pixel spacing) should then be preferred for more precise cartographic applications. Fine mode images display a lot of speckle, due to the one-look processing. However this does not generate confusion in stereo viewing and extraction because the human depth perception acts as a "filtering process".

Standard Mode Stereo Pair

Stereo pair 14 - RADARSAT - Sherbrooke, Québec, Canada

This stereo pair (S1/S4) is generated from descending path, standard mode images. It displays less cartographic detail due to a coarse resolution cell of about 26m in range by 27m in azimuth. For example, most of the roads are visible but with omission errors varying from 20% for main roads to 70% for "unclassified" city streets. However, the positioning accuracy is better than one resolution cell (Toutin, 1999). The four-look processing of the SAR data to generate the images has reduced the speckle but smoothed the linear features, which explains the larger omission errors. On the other hand, the oversampled image pixels, when compared to the SAR resolution cell explains the high positioning accuracy.

7.3 Processing Technique Examples

The following section is concerned with **simple image processing techniques** that can be done in order to allow a pair of images, which are not viewable in the raw image format, to be seen in stereo. Simple techniques such as resizing the images, allow us to print the images at the same approximate scale thus eliminating Y parallax. More complex techniques such as the slant range to ground range correction allow scale differences due to the slant range projection to be eliminated. A simple rotation allows the viewing of a stereo pair without having to rotate the images manually. Applying an antenna pattern correction allows the removal of the interfering effect of the antenna pattern. Finally, applying a filter to data allows some of the speckle in a image pair to be removed thereby increasing stereoviewability.

Image processing techniques involve resampling and/or radiometric transformation of the raw image. In order that too much information is not lost these techniques should be applied only when necessary.

7.3.1 Resizing Images

Stereo pair 10B - RADARSAT - Ottawa, Ontario, Canada

Too much Y parallax occurs in the S2/S3 and S1/S7 pairings of the raw Ottawa imagery. In these combinations, Y parallax is the result of differences in scale. The differences in scale between each image pair are 12.8 and 15.7 per cent respectively. As a general rule, scale differences greater than 10 percent in RADARSAT imagery will produce too great a Y parallax. The S1, S2 and S3 images have been re-scaled to the image dimensions of the S7 image. Once resized, any combination of these images can be successfully viewed in stereo.

7.3.2 Slant range to ground range correction to minimize scale differences

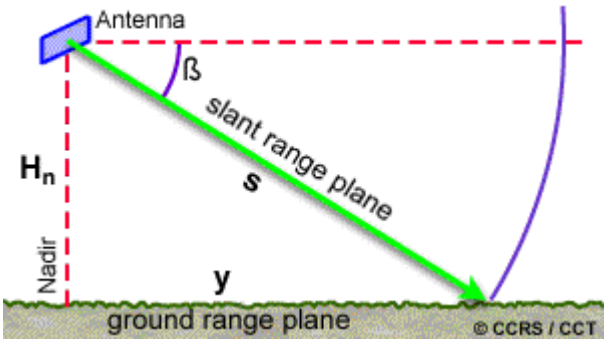

Slant versus Ground Range

Stereo pairs 16 & 16A - RADARSAT - Indonesia

An F5/F3 stereo pair is shown in slant range presentation. The images can be manually rotated with respect to each other in order to eliminate differences in orientation caused by the descending and ascending passes. The slant range presentation causes distortions in scale between the two images. The opposite side stereo configuration results in resolution differences. The most compressed near edges will be on the outer edge of the stereo pair, while the least compressed far edge is at the centre of the stereo-model. This means the same land features are resolved differently. This is particularly evident when the shorelines are examined. There is a great variation in shape between the two images. As a result of the slant range presentation and the opposite side stereo configuration, only small local areas of this image pair can be viewed in stereo.

This image pair is also difficult to view in stereo because there is very little elevation difference to perceive.

Stereo pairs 17 & 17A - RADARSAT - Indonesia

It is easier to see the stereo effect in Stereo pair 17 (than in Stereo pair 16). This is due to the ground range presentation of the image pair. But once again, rotation is still necessary for a better depth perception over a larger area . As these images are of flat terrain, the stereo effect is noticeable at the boundary between water and land. A slight slope leads down to the water's edge.

Radiometrically, both image pairs (16 and 17) show a very strong contrast between land and water, road network and surroundings on each image. There is very little variation between the images. Seasonal differences in vegetation are visible since there is a two-month difference between images.

7.3.3 Rotation

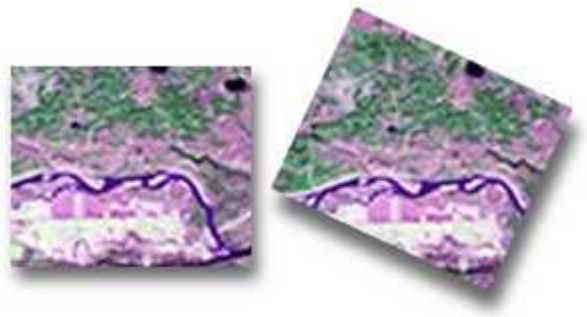

Stereo pair 1 - RADARSAT - Bathurst Island, Nunavut, Canada

Rotation of one image with respect to the other can be useful when the images are acquired over far northern or southern latitudes (greater than 60 degrees) or, when an opposite side stereo configuration is used to make up the stereo pair. For example, the

right hand image of Stereo pair 1 has been rotated with respect to the left-hand image using digital image analysis software.

Bathurst Island is at latitude 75 degrees North. In order to rotate the right hand image, common control points along the coastline were collected. The right hand image was then registered to the left using a first order polynomial transformation and a bilinear resampling kernel. This results in a right hand image that can be horizontally aligned with the left-hand image. Manual rotation is no longer necessary.

Stereo pair 11 - RADARSAT - Tapagos Forest, Brazil

In contrast, as the geographical location is just south of the Equator, the imagery of the Tapagos Forest, Brazil (Stereo pair 11) lines up without any manual rotation.

Stereo pair 17 - RADARSAT - Indonesia

Another example of imagery that could be digitally rotated in order to improve stereo viewability by eliminating the need for manual rotation is Stereo pair 17. Although this imagery of Indonesia is located at just 2 degrees South of the Equator, it has been acquired on an ascending and a descending pass. This causes the resulting two images to be rotated with respect to each other.

7.3.4 Radiometric Balancing

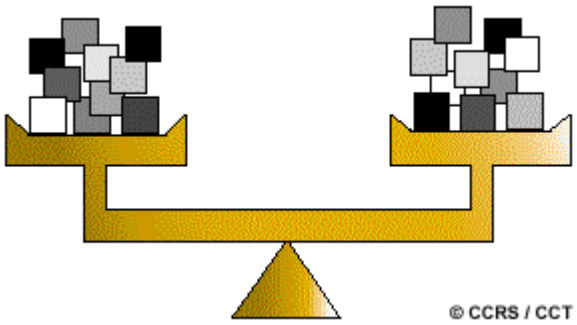

Radiometric balancing includes correction for a number of radiometric effects in radar imagery, including: antenna pattern, range (R3) fall-off, and systematic backscatter variation due to target distribution within an image.

Stereo pairs 18 & 18A - RADARSAT - Whitecourt, Alberta, Canada

Two versions of the right hand image (S1) are shown for comparison. The first S1 image is in its raw form, showing radiometric variability across the image. This variability is likely due to incomplete compensation for range-related variation in backscatter. A radiometric balancing correction has been applied to generate the second S1 image. It has also been rescaled to the image dimensions of the left-hand (S7) image.

This image pair is difficult to view in stereo. The processed S1 image improves stereo viewability of the image pair. In spite of the applied radiometric balancing and the rescaling, stereo can be viewed in local areas only. Manual rotation is necessary to capture approximately a quarter of a stereo-model at a time.

These images show a medium contrast between topographic features. Forest clear cuts are clearly visible, especially on the S7 image. Topographic features are much more pronounced on the S1 image. Foreshortening effects are also more apparent on the S1 image.

7.3.5 Filtering

Stereo pair 9A, 9B - RADARSAT - Okanagan Valley, British Columbia

As mentioned, RADARSAT data acquired in Fine mode is more prone to speckle than Standard mode data. To demonstrate the usefulness of applying a filter in order to increase stereo-viewability, an area of approximately 10x10 km of the Okanagan, B.C. data was prepared with and without a filter. The unfiltered version contains a large amount of speckle, which interferes with stereo viewing. An adaptive filter (Lopez et al., 1985) was then used to reduce the amount of speckle. This resulted in a cleaner image, which is easier to view in stereo. However, there is a loss of some detail. Roads and boundaries between water bodies and land are not as clearly delineated in the filtered image as in the unfiltered image. Some elevation information is also lost.

Bibliography

Agnard, J.P., P.-A. Gagnon, and C. Nolette, 1988, **Microcomputers and Photogrammetry A New Tool: The Videoplotter**, Photogrammetric Engineering and Remote Sensing, Vol. 54, No. 8, pp.1165-1167.

Benis, S. V., J. L. Leeds, and E. A. Winer, 1988, **Operator Performance as a Function of Type of Display: Conventional versus Perspective**, Human Factors, Vol. 30, pp. 162-169.

Benton, S. A., D. A. Duston-Roberge, and R. Simard, 1985, **A Chromatic Holographic Stereogram of Landsat MSS Data**, Optical Engineering, Vol. 24, No. 2, pp. 338-340.

Braunstein, M. L., 1976, **Depth Perception Through Motion**, Academic Press, Inc., New York, N.Y., 206 pages.

Denyer, N., R. K. Raney and N. Shepherd, 1993, **The SAR Data processing Facility**, Canadian Journal of Remote Sensing, Vol. 19, No. 4, pp. 311-316.

Dowman, I.J., H. Ebner and C. Heipke, 1992. **Overview of European developments in digital photogrammetric workstations**, Photogrammetric Engineering and Remote Sensing, 58 (1), 51-56.

Einthoven, W., 1885 **Stereoscopie durch Farbendifferenz**, Albrecht von Graefes Archiv fur Opthamologie, Vol. 31, pp. 211-238.

Elachi, C., 1987, **Introduction to the Physics and Techniques of Remote Sensing**, John Wiley and Sons, Inc., New York, N.Y., 413 pages.

Friedhoff, R. M. and W. Benzon, 1991, **The Second Computer Revolution: Visualization**, W.H. Freeman and Company, New York, N.Y., 215 pages.

Fullerton, J. K., F. W. Leberl, and R. E. Marque, 1986, **Opposite-Side SAR Image Processing for Stereo Viewing**, Photogrammetric Engineering and Remote Sensing, Vol. 52, No. 9, pp. 1487-1498.

Gabor, D., 1948, **A New Microscopic Principle**, Nature, Vol. 761, No.161, pp. 777-779.

Gagnon, P.-A., J. P. Agnard, C. Nolette, and M. Boulianne, 1990, **A Microcomputer-Based General Photogrammetric System**, Photogrammetric Engineering and Remote Sensing, Vol. 56, No. 5, pp. 623-625.

Heipke, C., 1995, **State-of-the-art Digital Photogrammetric Workstations for Photogrammetric Applications**, Photogrammetric Engineering and Remote Sensing, Vol. 61, No. 1, pp. 49-56.

Helava, U. V., 1988, **On System Concepts for Digital Automation**, International Archives of Photogrammetry and Remote Sensing, Vol. 27, V2 , pp. 171-190.

Jones, E. R., A. P. McLaurin, and L. Cathey, 1984, **VISIDEP TM: Visual Image Depth Enhancement by Parallax Induction**, Proceedings Society of Photo-Optical Instrumentation Engineers, Advances in display technology IV (E. Schalm, Editor), SPIE, Vol. 457, pp. 16-19.

Leberl, F. W., 1990, **Radargrammetric Image Processing**, Artech House, Norwood, Ma. 590 pages.

Leonardo, E. S., 1983, **Stereo Models from Synthetic Aperture Radar**, Proceedings of Conference on Extraction of Information from Remotely Sensed Images, Rochester, N.Y., August 16-19, pp. 105-114.

Lillesand, T. M. and Kiefer, R. W., 1987, **Remote Sensing and Image Interpretation**, John Wiley and Sons, Inc., New York, N.Y., 721 pages.

Lopes, A., R. Touzi and E. Nezry, 1990, **Adapative speckle filters and scene heterogeneity**, IEEE Trans. Geosc. Remote Sensing, Vol. 28, No. 6, pp. 992-1000.

Luscombe, A. P., I. Ferguson, N. Shepherd, D.G. Zimcik, and P. Naraine, 1993, **The RADARSAT Synthetic Aperture Radar Development**, Canadian Journal of Remote Sensing, Vol. 19, No. 4, pp. 298-310.

Mattas, R. B., J. C. Townsend, and H. W. Leibowitz, 1978, **Some Effects of Chromostereopsis on Stereoscopic Performance: Implications for Microscopes**, Human Factors, Vol. 20, No. 4, pp. 401-408.

McLaurin, A. P., E. R. Jones, L. Cathey, 1988, **Advanced Alternating-Frame Technology (VISIDEP TM) and Three-Dimensional Remote Sensing**, IEEE Transactions on Geoscience and Remote Sensing, Vol. 26, No.4, pp. 437-440.

Moore, J., J.E. Shepphard, J. Pizzacaroli, and P. Lyman, 1993, **RADARSAT: Spacecraft Bus and Solar Array**, Canadian Journal of Remote Sensing, Vol. 19, No. 4, pp. 289-297.

Okoshi, T., 1976, **Three-dimensional Imaging Techniques**, Academic Press Inc., New York, N.Y., 403 pages.

Parashar, S., E. Langham, J. McNally, and S. Ahmed, 1993, **RADARSAT Mission Requirements and Concept**, Canadian Journal of Remote Sensing, Vol. 19, No. 4, pp. 280-288.

RADARSAT International, 1995, **RADARSAT Illuminated**

Simonet, P., and M. Campbell, **Effect of illuminance on the directions of chromostereopsis and transverse chromatic abberation observed with natural pupils**, Ophthamological and Physiological Optics, Vol. 10, July 1990, pp. 271-279.

Simple Anatomy of the Retina http://webvision.med.utah.edu/sretina.html.

Slama, C. C. (Editor-in-Chief), 1980, **Manual of Photogrammetry**, American Society of Photogrammetry, Falls Church, Va., 4th Edition, 1056 pages

Steenblik, R. A., 1987, **The chromo-stereoscopic process: a novel single image stereoscopic process**, True 3-D Imaging Display Techniques and Display Technologies, SPIE, Vol. 761

Steenblik, R. A., 1986, 1991, **Stereoscopic Process and Apparatus Using Different Deviations of Different Colors**, U.S. Patents No. 4-597-634 and 5-002-364.

Toutin, Th. and M. Beaudoin, 1995, **"Real-time extraction of planimetric and altimetric features from digital stereo SPOT data using a digital video plotter"**, Photogrammetric Engineering and Remote Sensing, Vol. 61, No. 1, pp. 63-67.

Toutin, Th. and B. Rivard, 1995, **A new tool for depth perception of multi-source data**, Photogrammetric Engineering and Remote Sensing, Vol. 61, No. 10, pp.1209-1211.

Toutin, Th. and B. Rivard, 1997, **Value-added RADARSAT Products for Geoscientific Applications**, Canadian Journal of Remote Sensing, Vol 23, No.1, pp. 63-70.

Toutin, Th., 1995, **Airborne SAR Stereo Restitution in a Mountainous Area of Costa Rica: First Results**, IEEE Transactions on Geoscience and Remote Sensing. Vol. 33, No.2, pp. 500-504.

Toutin, Th., 1996, **Opposite Side ERS-1 Stereo Mapping over Rolling Topography**, IEEE Transactions on Geoscience and Remote Sensing. Vol. 34, No.2, pp. 543-549.

Toutin, Th., 1997 a, **Qualitative aspect of chromo-stereoscopy for depth perception**, Photogrammetric Engineering and remote Sensing, Vol. 65, No. 2, pp. 193-203.

Toutin, Th., 1997 b, **Accuracy Assessment of Stereo-Extracted data from Airborne SAR Images**, International Journal of Remote Sensing, Vol. 18, No.18, pp. 3693-3707.

Toutin, Th., 1997 c, **SPOT and Landsat Stereo Fusion for Data Extraction over mountainous Areas**, Photogrammetric Engineering and Remote Sensing, Vol. 64, No.2, pp. 109-113.

Toutin, Th., 1997 d, **Single versus stereo ERS-1 SAR imagery for planimetric feature extraction**, International Journal of Remote Sensing, Vol. 18, No.18, pp. 3909-3914.

Toutin, Th., 1998 a, **3D Data Stereoscopic Extraction from Mixed VIR and SAR Sensors**, Proceedings of the 20th Remote Sensing Symposium, Calgary, AB, May 10-13, 1998, pp. 239-242.

Toutin, Th., 1998 b, **Stereo RADARSAT for Mapping Applications**, Proceedings of the 2nd International ADRO Symposium "Bringing Radar Applications Down to Earth", Montreal, Québec, Canada, October 13-15, CDROM.

Toutin, Th., 1999, **Road Extraction from RADARSAT Data**, Proceedings of the 19th International Cartographic Conference, Ottawa, Ontario, Canada, August 14-21, CDROM.

Usery, L., 1993, **Virtual Stereo Display Techniques for Three-dimensional Geographic Data**, Photogrammetric Engineering and Remote Sensing, Vol. 59, No. 12, pp. 1737-1744.

Walko, J., 1995, **Sharp Claims Advance in 3-D Moving Images**, Photonics Spectra, Vol. 29, No.3, pp.28-29.

Wolf, P. R., 1983, **Elements of Photogrammetry**, McGraw-Hill, Inc., New York, N.Y., 628 pages.

Ye, M., A. Bradley, L. N. Thibos, and X. Zhang, 1992, **The effect of pupil size on chromostereopsis and chromatic diplopia: Interaction between the Stiles-Crawford effect and chromatic aberrations**, Vision Research, Vol. 32, No. 11, pp. 2121-2128.

Acknowledgements

The authors, Dr. Thierry Toutin and Corinna Vester would like to thank the following people and organizations for various contributions made to the development of this tutorial:

- The Multimedia Applications Section of CCRS
- Marc D'Iorio, Vern Singhroy, Ridha Touzi, Frank Ahern
- Julie Allard, Carolin Jans, Daniel Alvarez
- The GlobeSAR project team of CCRS
- John van Genderen and Christine Pohl of ITC (Netherlands)
- RADARSAT International Inc.
- The Canadian Space Agency
- Sylvana Amaral (INPE, Brazil)

Image Data Credits

- RADARSAT data - © CSA/ASC 1996 - Received by CCRS and Processed by RADARSAT International Inc.
- SPOT data - © CNES, 1990 - Received and distributed by CCRS
- Landsat data - © EOSAT 1993 - Received and distributed by CCRS
- ERS-1 data - © ESA/ASE 1992 - Received and distributed by CCRS
- JERS-1 data - © NASDA 1993 - Courtesy of ITC, the Netherlands
- Airborne SAR data - Acquired and processed by CCRS

- Aerial Photos © NRCan - Acquired from the National Air Photo Library
- Ground Photos - Tom Alföldi